William & Mary
CHARTERED 1693

W&M ScholarWorks

VIMS Articles | Virginia Institute of Marine Science

9-13-2018

Future response of global coastal wetlands to sea-level rise

M. Schuerch

T. Spencer

S. Temmerman

Matthew L. Kirwan
Virginia Institute of Marine Science

et al

Follow this and additional works at: https://scholarworks.wm.edu/vimsarticles

Part of the Environmental Sciences Commons

Recommended Citation

Schuerch, M.; Spencer, T.; Temmerman, S.; Kirwan, Matthew L.; and al, et, "Future response of global coastal wetlands to sea-level rise" (2018). *VIMS Articles*. 1296.
https://scholarworks.wm.edu/vimsarticles/1296

This Article is brought to you for free and open access by the Virginia Institute of Marine Science at W&M ScholarWorks. It has been accepted for inclusion in VIMS Articles by an authorized administrator of W&M ScholarWorks. For more information, please contact scholarworks@wm.edu.

Future response of global coastal wetlands to sea level rise

Mark Schuerch[1,2*], Tom Spencer[2], Stijn Temmerman[3], Matthew L. Kirwan[4], Claudia Wolff[5], Daniel Lincke[6], Chris J. McOwen[7], Mark D. Pickering[8], Ruth Reef[9], Athanasios T. Vafeidis[5], Jochen Hinkel[6,10], Robert J. Nicholls[11], Sally Brown[11]

[1] Lincoln Centre for Water and Planetary Health, School of Geography, University of Lincoln, Lincoln, United Kingdom

[2] Cambridge Coastal Research Unit, Department of Geography, University of Cambridge, Cambridge United Kingdom

[3] Ecosystem Management Research Group, University of Antwerp, Antwerp, Belgium

[4] Virginia Institute of Marine Science, College of William and Mary, Gloucester Point, Virginia, USA

[5] Institute of Geography, Christian-Albrechts University of Kiel, Kiel, Germany

[6] Global Climate Forum, Berlin, Germany

[7] UN Environment World Conservation Monitoring Centre, Cambridge, United Kingdom

[8] Ocean and Earth Science, National Oceanography Centre, University of Southampton, Southampton, United Kingdom

[9] School of Earth, Atmosphere and Environment, Monash University, Clayton, Victoria, Australia

[10] Division of Resource Economics, Thaer-Institute and Berlin Workshop in Institutional Analysis of Social-Ecological Systems (WINS), Humboldt-University, Berlin, Germany

[11] Faculty of Engineering and the Environment, University of Southampton, Southampton, United Kingdom

*Corresponding author: mschuerch@lincoln.ac.uk

Introduction

The response of coastal wetlands to sea level rise (SLR) during the 21st century remains uncertain. Global-scale projections suggest that between 20% and 90% (for low and high SLR scenarios, respectively) of the present-day coastal wetland area will be lost, including the loss of biodiversity and highly valued ecosystem services[1-3]. These projections do not necessarily take into account all essential geomorphological[4-7] and socio-economic system feedbacks[8]. Here we present an integrated global modelling approach that considers (i) the ability of coastal wetlands to build up vertically by sediment accretion and (ii) the accommodation space, namely the vertical and lateral space available for fine sediments to accumulate and to be colonised by wetland vegetation. We use this approach to assess global-scale changes in coastal wetland area in response to global SLR and anthropogenic coastal occupation during the 21st century. Based on our simulations we find that, globally, wetland gains of up to 60% of the current area are expected, if more than 37% of coastal wetlands have sufficient accommodation space, and sediment supply remains at present levels. In contrast to previous studies[1-3], we project that until 2100 global coastal wetland loss will range between 0% and 30%, assuming no additional accommodation space. Our simulations suggest that global wetland resilience is primarily driven by the availability of accommodation space, which is strongly influenced by the building of anthropogenic infrastructure in the coastal zone and its expected to change over the 21st century. Rather than being an inevitable consequence of global SLR, our findings indicate that large-scale coastal wetland loss might be avoidable, if sufficient additional accommodation space can be created through innovative "nature-based adaptation" solutions to coastal management.

Main text

Coastal wetlands provide many important ecosystem services (valued up to 194,000 USD ha^{-1} yr^{-1})[9], including carbon sequestration[10-11], natural coastal protection[12-15], support of fisheries[16] and water quality improvement[17]. Recent global-scale assessments of coastal wetland dynamics have suggested that the ability of many marshes and mangroves to build up vertically has already been overwhelmed by present-day SLR, leading to widespread wetland loss[1-3]. At the same time, more regional to local-scale field measurements and models of salt marsh accretion have concluded that most large-scale assessments have overestimated the vulnerability of coastal wetlands to SLR[4]. These differences highlight a major knowledge gap in our understanding of coastal wetland responses to global environmental change. It has been argued that the reason for the observed discrepancy is that large-scale assessments have so far failed to consider the well-understood bio-physical feedback mechanisms which are typically included in local-scale models[4]. These mechanisms include the ability of coastal wetlands to build up vertically by sediment accretion which is enhanced with increasing inundation heights and frequencies, triggered for example by accelerating SLR, and which enables coastal wetlands to persist or even prosper with SLR[5-7].

A second limitation of previous global-scale assessments is that they have not yet represented accommodation space (the vertical and lateral space available for fine sediments to accumulate and be colonised by wetland vegetation) in a spatially explicit manner[2,4]. This constitutes an important gap as recent papers have suggested that anthropogenic barriers to inland wetland migration (coastal flood protection structures, coastal roads and railway lines, settlements, and impervious land surfaces) may be a more important threat to coastal wetlands than drowning by SLR alone[2,4,18].

We address both of these limitations, and assess global-scale changes in coastal wetland area in response to global SLR and anthropogenic coastal occupation, using a novel integrated modelling approach. For the first time, we consider (1) the vertical adaptability of coastal wetlands by bio-physical feedbacks between wetland accretion and SLR, assuming current-day levels of sediment availability, and (2) their horizontal adaptability, as determined by the interactions between inland wetland migration and anthropogenic barriers, assuming wetland inland migration to be a function of accommodation space[8]. We present a model to make projections of the global resilience of coastal wetlands to 21st century SLR scenarios under existing and increased accommodation space, representing present conditions and two additional coastal management scenarios following the wider implementation of nature-based adaptation strategies[12]. By means of a comprehensive sensitivity analysis, we finally assess the extent to which this resilience is controlled by vertical and horizontal adaptation mechanisms.

Based on the simulation runs during model calibration, our calibrated model, which includes mangroves, salt and freshwater tidal marshes, correctly predicts observations of present-day vertical wetland change, obtained from large meta-datasets from all over the world[3,4,19], for 78% of all coastal areas where data is currently available (N=46) (ED Table1, ED Fig.1). While performing very well in regions where coastal wetlands were reported to be stable (i.e. with vertical wetland growth in balance with local SLR) or drowning (i.e. slower vertical wetland growth than local SLR), our model tends to underestimate the number of locations with an elevation surplus (i.e. faster vertical wetland growth than local SLR). Hence our predictions of the ability of wetlands to vertically grow in pace with 21st century SLR rates may be considered conservative.

Projections of the future extent of coastal wetlands by 2100 are based on simulations using three different regionalized relative SLR scenarios (RCPs 2.6, 4.5 and 8.5 corresponding to a SLR of 29, 50 and 110 cm by 2100) and three human adaptation scenarios with varying degrees of available accommodation space (ED Table2): i) business-as-usual (BAU) scenario in which we assume that no accommodation space is available where local population densities in the 1-in-100 year coastal floodplain exceed thresholds between 5 and 20 people km^{-2}; ii) moderate level of nature-based adaptation (NB 1) in which the population density threshold ranges between 20 and 150 people km^{-2} and iii) high level of nature-based adaptation (NB 2) with population density thresholds between 150 and 300 people km^{-2}. Changes in population growth during the simulation period are considered by applying a scenario of national population growth rates based on the shared socio-economic pathway SSP2 (IIASA)[20], which is characterized by a moderate, and after 2070 slowing, global population growth leading to 9 billion people by 2100[21].

Under all SLR scenarios, 20 people km^{-2} constitutes a critical population density threshold. If a higher population density threshold is applied, more coastal wetlands have sufficient accommodation space to migrate inland resulting in an overall gain in global coastal wetland area (Fig. 1). If lower thresholds are considered, less coastal wetlands have sufficient accommodation space resulting in an overall global loss. The population density threshold of 20 people km^{-2} corresponds to what we estimate as the current global average above which coastal communities are protected by some kind of coastal protection infrastructure (Supplementary Information), hence allowing inland migration for only 37% of all global coastal wetlands. A population density threshold of 300 people km^{-2} is the lower threshold for urban developments, as defined by the European Commission[22], and sets the upper limit for potential wetland inland migration (NB 2 scenario). The highest SLR scenario at this threshold results in a substantial increase in global coastal wetland area (+60%). The same SLR scenario with a threshold population density of 5 people km^{-2} results in a net global loss of 30% (Fig. 1). When applying the lowest SLR scenario, areal coastal wetland changes for population density thresholds between 5 and 300 people km^{-2} only range between -8% (loss) and +15% (gain) (Fig. 1). The largest changes are observed for mangroves, which make the largest contribution to the global wetland area from the beginning (69%). Interestingly, hardly any losses are observed for salt marshes, even under the human adaptation scenarios with the least accommodation space (Fig. 1).

Under the business-as-usual (BAU) scenario for accommodation space (5-20 people km^{-2}), changes in the extent of global coastal wetlands range between -8% (loss) and 0% (no change) for the lowest SLR scenario and between -30% (loss) and -8% (loss) for the highest SLR scenario. These losses can primarily be attributed to an increasing sediment deficiency, impeding the wetland's ability to vertically keep pace with SLR. If, in the future, coastal wetlands are given more accommodation space (e.g. in the context of the implementation of nature-based adaptation solutions), global coastal wetlands could increase in areal extent (Fig. 1). Our moderate nature-based adaptation scenario (NB 1: 20-150 people km^{-2}) results in an increase between 0% and 12% for the low, and between -8% (loss) and 42% for the high, SLR scenario. Under the more extreme adaptation scenario (NB 2: 150-300 people km^{-2}) we anticipate even higher increases, between 12% and 15% for the low, and between 42% and 60% for the high, SLR scenario (Fig. 1). In contrast to the BAU scenario, these gains for the moderate and extreme nature-based adaptation scenarios (NB 1 and NB 2) are driven by inland wetland migration rather than vertical sediment accretion, therefore independent of sediment availability.

Under the BAU scenario (lower boundary: 5 people km^{-2}), the majority of the absolute loss in coastal wetland areas (ca. 66%) is projected to occur in the Caribbean Sea, the southern US east coast and parts of south-east Asia (Fig. 2a). Similarly, Lovelock et al.[19] identified south-east Asia as a highly critical region for mangrove resilience to SLR. The patterns of expected relative changes in wetland areas (i.e. percent gain or loss) are somewhat different but essentially confirm the model results of Spencer et al.[2]; largest relative area losses (again, under a scenario of highly constrained accommodation space) are found in the Caribbean Sea, along the eastern US coast as well as in the western Baltic Sea, the Mediterranean Sea, the Red Sea and in parts of south-east Asia (Fig. 2b).

The spatial patterns of coastal wetland loss strongly resemble those of the modelled present-day sediment balance, namely the difference between the sediment required for a coastal wetland surface to keep pace vertically with current local relative SLR and the current-day sediment availability (Fig. 3). For example, large regions of sediment deficit are identified in the Caribbean Sea, western Baltic Sea, Mediterranean Sea, and along the US east and west coasts (Fig. 3). These areas largely coincide with the hotspot regions for relative wetland area losses under a scenario of highly constrained accommodation space (Fig. 2). Meanwhile, most parts of Asia, South America and

North-West Europe show sufficient or excess sediment availability (Fig. 3) which correspond to areas with small relative wetland loss, even where accommodation space is limited, as vertical sediment accretion counteracts relative SLR (Fig. 2a).

Our sensitivity analysis confirms the importance of accounting for vertical sediment accretion with our "sediment accretion only" scenario (scenario HYS 2, ED Table2). This scenario reduces the global loss of coastal wetlands from 38% to 20%, 50% to 26% and 77% to 54% for the low, medium and high SLR scenarios respectively, as compared to our "no resilience" scenario where no accommodation space and no vertical sediment accretion is assumed (scenario HYS 4, ED Table2, ED Fig.2).

Previous studies have highlighted the dangers of low sediment availability and reduced sediment supply, threats that may be exacerbated regionally by increasing numbers of dams being built within river catchments, causing increased risk for coastal wetland loss with SLR[24-26]. However, our model sensitivity analysis under the high SLR scenario (RCP 8.5), and accounting for vertical sediment accretion, demonstrates that if present-day values of sediment supply were to change by +/-50%, only a ±6% change in global wetland area would result (ED Table3). In contrast, accommodation space for inland wetland migration has a much stronger control on wetland persistence with SLR, yet much less is known about the actual process and further research is urgently needed. Our sensitivity analysis shows that even in heavily sediment-starved regions, an increase in accommodation space could result in a net wetland gain (ED Fig.3), particularly under high rates of SLR, even though the wetland's seaward side could regularly be lost due to the lack of sediment. Under extreme rates of SLR, and where sediment availability is insufficient, future coastal wetlands may therefore have a shorter lifetime and a lower degree of geomorphological, hydrological and biogeochemical complexity[27].

It should be noted that locally and especially in delta regions, these global mechanisms may not be as straight forward because historical and contemporary catchment and delta practices (e.g. river damming and dredging) are responsible for much of the observed coastal wetland trends in many "loss hotspots" rather than global SLR[26]. Also, constraints on the inland migration of coastal wetlands may arise from adverse soil conditions, particularly where the inundated land has been intensively modified by humans, unsuitable geomorphological characteristics or elevation constraints (if located too low in the tidal frame)[27,28]. In order to alleviate these constraints, coastal management strategies and engineering may locally be required to facilitate coastal wetlands to migrate inland[27]. As a consequence, local patterns of wetland resilience may be at considerable variance with global estimates of change.

Our model projections suggest that nature-based adaptation solutions that maximise the inland migration of tidal wetlands in response to SRL, wherever possible, may help safeguard wetland persistence with SLR and protect associated ecosystem services. Existing nature-based adaptation solutions that allow coastal wetlands to migrate inland include the inland displacement of coastal flood defences (typically along highly engineered coastlines)[12] or the designation of nature reserve buffers in upland areas surrounding coastal wetlands[18]. These schemes, however, are currently implemented as local-scale projects only; strategically upscaling such projects, such as for example suggested by the so-called shoreline management plans in England and Wales[29] or the Coastal Master Plan in Lousiana[30] may help coastal wetlands adapt to SLR at the landscape scale and protect rapidly increasing global coastal populations.

References

1 Blankespoor, B., Dasgupta, S. & Laplante, B. Sea-Level Rise and Coastal Wetlands. *Ambio* **43**, 996-1005 (2014).

2 Spencer, T. *et al.* Global coastal wetland change under sea-level rise and related stresses: The DIVA Wetland Change Model. *Global and Planetary Change* **139**, 15-30 (2016).

3 Crosby, S. C. *et al.* Salt marsh persistence is threatened by predicted sea-level rise. *Estuarine, Coastal and Shelf Science* **181**, 93-99 (2016).

4 Kirwan, M. L., Temmerman, S., Skeehan, E. E., Guntenspergen, G. R. & Fagherazzi, S. Overestimation of marsh vulnerability to sea level rise. *Nature Climate Change* **6**, 253-260 (2016).

5 Schuerch, M., Vafeidis, A., Slawig, T. & Temmerman, S. Modeling the influence of changing storm patterns on the ability of a salt marsh to keep pace with sea level rise. *Journal of Geophysical Research: Earth Surface* **118**, 84-96 (2013).

6 French, J. R. Numerical simulation of vertical marsh growth and adjustment to accelerated sea-level rise, North Norfolk, U.K. *Earth Surface Processes and Landforms* **18**, 63-81 (1993).

7 Morris, J. T., Sundareshwar, P. V., Nietch, C. T., Kjerfve, B. & Cahoon, D. R. Responses of coastal wetlands to rising sea level. *Ecology* **83**, 2869-2877 (2002).

8 Enwright, N. M., Griffith, K. T. & Osland, M. J. Barriers to and opportunities for landward migration of coastal wetlands with sea-level rise. *Frontiers in Ecology and the Environment* **14**, 307-316 (2016).

9 Costanza, R. *et al.* Changes in the global value of ecosystem services. *Global Environmental Change* **26**, 152-158 (2014).

10 Duarte, C. M., Losada, I. J., Hendriks, I. E., Mazarrasa, I. & Marba, N. The role of coastal plant communities for climate change mitigation and adaptation. *Nature Climate Change* **3**, 961-968 (2013).

11 McLeod, E. *et al.* A blueprint for blue carbon: toward an improved understanding of the role of vegetated coastal habitats in sequestering CO2. *Frontiers in Ecology and the Environment* **9**, 552-560 (2011).

12 Temmerman, S. *et al.* Ecosystem-based coastal defence in the face of global change. *Nature* **504**, 79-83 (2013).

13 Möller, I. *et al.* Wave attenuation over coastal salt marshes under storm surge conditions. *Nature Geoscience* **7**, 727-731 (2014).

14 Shepard, C. C., Crain, C. M. & Beck, M. W. The protective role of coastal marshes: a systematic review and meta-analysis. *PLOS ONE* **6**, e27374 (2011).

15 Stark, J., Van Oyen, T., Meire, P. & Temmerman, S. Observations of tidal and storm surge attenuation in a large tidal marsh. *Limnology and Oceanography* **60**, 1371-1381 (2015).

16 Aburto-Oropeza, O. *et al.* Mangroves in the Gulf of California increase fishery yields. *Proceedings of the National Academy of Sciences* **105**, 10456-10459 (2008).

17 Teuchies, J. *et al.* Estuaries as filters: the role of tidal marshes in trace metal removal. *PLOS ONE* **8**, e70381 (2013).

18 Kirwan, M. L. & Megonigal, J. P. Tidal wetland stability in the face of human impacts and sea-level rise. *Nature* **504**, 53-60 (2013).

19 Lovelock, C. E. *et al.* The vulnerability of Indo-Pacific mangrove forests to sea level rise. *Nature* **526**, 559-563 (2015).

20 van Vuuren, D. P. *et al.* A new scenario framework for climate change research: scenario matrix architecture. *Climatic Change* **122**, 373-386 (2014).

21 KC, S. & Lutz, W. The human core of the shared socioeconomic pathways: Population scenarios by age, sex and level of education for all countries to 2100. *Global Environmental Change* **42**, 181-192 (2017).

22 Dijkstra, L. & Poelman, H. *A harmonised definition of cities and rural areas: the new degree of urbanisation.* (European Commission, 2014).

23 Day, J. W., Pont, D., Hensel, P. F. & Ibàñez, C. Impacts of sea-level rise on deltas in the Gulf of Mexico and the Mediterranean: The importance of pulsing events to sustainability. *Estuaries* **18**, 636-647 (1995).

24 Yang, S. L. *et al.* Impact of dams on Yangtze River sediment supply to the sea and delta intertidal wetland response. *Journal of Geophysical Research: Earth Surface* **110**, F03006 (2005).

25 Ganju, N. K. *et al.* Spatially integrative metrics reveal hidden vulnerability of microtidal salt marshes. *Nature Communications* **8**, 14156 (2017).

26 Jankowski, K. Törnqvist, T. E. & Fernandes, A. M. Vulnerability of Louisiana's coastal wetlands to present-day rates of relative sealevel rise, *Nature Communications* **8**, 14792. (2017).

27 Spencer, K. L. *et al.* Physicochemical changes in sediments at Orplands Farm, Essex, UK following 8 years of managed realignment. *Estuarine, Coastal and Shelf Science* **76**, 608-619 (2008).

28 French, P. W. Managed realignment - The developing story of a comparatively new approach to soft engineering. *Estuarine, Coastal and Shelf Science* **67**, 409-423 (2006).

29 Nicholls, R. J., Townend, I. H., Bradbury, A. P., Ramsbottom, D. & Day, S. A. Planning for long-term coastal change: Experiences from England and Wales. *Ocean Engineering* **71**, 3-16 (2013).

30 Peyronnin, N. *et al.* Louisiana's 2012 Coastal Master Plan: Overview of a Science-Based and Publicly Informed Decision-Making Process. *Journal of Coastal Research* **SI67**, 1-15 (2013).

Acknowledgement

This research was financially supported by the 'Deutsche Forschungsgemeinschaft' (DFG) through the Cluster of Excellence 80 'The Future Ocean', funded within the framework of the Excellence Initiative on behalf of the German federal and state governments, the personal research fellowship of Mark Schuerch (Project Number 272052902) and by the Cambridge Coastal Research Unit (Visiting Scholar Programme). Furthermore, this work has partly been supported by the EU research project RISES-AM- (FP7-ENV-693396).

We thank M. Martin for support in editing the calibration data and G. Amable for valuable statistical advice.

Author contributions

M.S., T.S. developed the model algorithm. M.S., D.L. developed the model code. M.S., C.W., C.McO., M.D.P., M.L.K., A.T.V., R.R., S.B. gathered/produced input data. M.S., S.T., R.J.N. analysed / interpreted the model simulations. M.S., T.S., S.T. M.L.K., J.H. wrote the paper.

Author information

The authors declare no competing interests.

Figure legends

Figure 1: Global change (km^2) in coastal wetland areas. Results are displayed for all three SLR scenarios (RCP 2.6 - low, RCP 4.5 - medium, RCP 8.5 - high) and three human adaptation scenarios, defined by different population density thresholds (BAU 1: 5 - 20 people km^{-2}, NB 1: 20 - 150 people km^{-2}, NB 2: 150 - 300 people km^{-2}). Sediment accretion is considered, and wetland inland migration

is limited to where the population density in the 1-in-100 year floodplain falls below the respective threshold. Areal changes of all three wetland types are indicated in the tables below the graphs.

Figure 2: Spatial distribution of coastal wetland change. Absolute (a) and relative (b) changes in coastal wetland areas are displayed for the medium SLR scenario (RCP4.5 (med)), assuming inhibition of wetland inland migration everywhere, but in (nearly) uninhabited regions with a population density <5 people km^{-2}. Population density is subject the population growth throughout the simulation period, following the shared socio-economic pathway SSP2[21,22]. The displayed coastline was generated during the DINAS-COAST FP5-EESD EU project (EVK2-CT-2000-00084).

Figure 3: Present-day global sediment balance. Sediment surplus (positive values) or sediment deficits (negative values) (in mg l^{-1}) represent the difference between the sediment concentration needed for coastal wetlands to vertically build up with current SLR rates and the actual sediment concentration derived from the satellite-borne Globcolour data (http://globcolour.info). The displayed coastline was generated during the DINAS-COAST FP5-EESD EU project (EVK2-CT-2000-00084).

Methods

General description of Model approach

Our model is based on the construction of coastal profiles for 12,148 coastline segments. These segments constitute the spatial units of the *Dynamic Interactive Vulnerability Assessment* (DIVA) modelling framework[31,32]. The coastal profiles are derived from the Shuttle Radar Topography Mission (SRTM) floodplain data, available from the global DIVA database[33]. Within each coastline segment, the existing coastal wetlands, as reported by the United Nations Environment Programme World Conservation Monitoring Centre (UNEP WCMC)[34,35], are assumed to be located between mean sea level (MSL) and mean high water spring (MHWS) level. With SLR, the seaward side of the wetlands are increasingly inundated ("unconstrained wetland loss"), while the landward side migrates inland by converting terrestrial uplands to coastal wetlands (Figs. ED1, ED2)[36]. However, inland wetland migration may be inhibited by anthropogenic coastal infrastructure reducing the available accommodation space[36-39], a variable that we approximate with the population density in the floodplain of the 1-in-100 year extreme water level (ED Fig.4).

Seaward wetland loss through inundation is counteracted by a large tidal range and a high sediment availability, as both these variables increase the resilience of coastal wetlands towards drowning through vertical sediment accretion processes[19,40-44]. This is represented by the Wetland Adaptability Score (WAS) reducing the loss of wetlands where tidal range and sediment availability are high[40] (ED Fig.4). The calculation of the WAS is based on a linear relationship between sediment availability and wetland drowning, whereas the slope of the linear relationship depends on tidal range. This relationship was suggested by Kirwan et al.[40], who ran an ensemble of five different tidal marsh accretion models to identify the critical rates of relative SLR as a function of tidal range and sediment availability.

Following the calculation of the seaward wetland loss and inland wetland gain, the resulting global coastal wetland areas are calculated for every model time step (5 years) between 2010 and 2100.

The model is driven by temporal changes in the model variables "Regional relative sea level rise" and "Population density" according to a range of regionalized scenarios for global SLR (Representative Concentration Pathways: RCPs)[45] and the shared socio-economic pathway SSP2[20] for national population growth respectively (ED Table2, ED Fig.4).

Input data

Database and data model

The input variables are derived from spatially explicit global datasets. They are attributed to the 12,148 coastline segments, which have an average length of 57 km[31]. Coastline segmentation is a product of the DIVA modelling framework; the related database includes more than 100 bio-physical and socio-economic parameters[31]. The dissection of the global coastline into segments is based on the concept of McFadden et al.[46], where coastal units have been created such that bio-physical and socio-economic impacts of global SLR are expected to be comparable within each coastline segment.

Construction of the coastal topographic profile

For each of the DIVA coastline segments, the coastal topographical profile is approximated using the areal information on coastal floodplains taken from Hinkel et al.[32]. They provide floodplain areas (km^2) for the elevation increments <1.5 m, 1.5-2.5 m, 2.5-3.5 m, 3.5-4.5 m, 4.5-5.5 m, 5.5-8.5 m, 8.5-12.5 m, 12.5-16.5 m, based on freely available Shuttle Radar Terrain Mission (SRTM) data[47]. The SRTM data has a 90 m horizontal and a 1 m vertical resolution. The coastal profiles are constructed by dividing the floodplain areas per elevation increment by the length of the corresponding coastline segment in order to calculate the inundation lengths, which are then plotted against the upper boundaries of the elevation increments (i.e. 1.5 m, 2.5 m, 3.5 m, etc.) (ED Fig.5). It is thereby assumed that elevations continuously increase with distance from the coast, which has been shown to be a reasonable assumption[33].

Elevations between the upper boundaries of the elevation increments are linearly interpolated following earlier global assessments[32,48-50]. Titus and Richman[51] and Titus and Wang[52] who linearly interpolated between the MHWS level and an elevation of 1.5 m (or higher) showed that their method approximated high resolution LIDAR-derived elevations with a mean error of less than 30 cm and that linear interpolation produces no systematic bias with respect to the area of inundated land, even for the lowest 50 cm of the profile[52].

Wetland data

The areal wetland extents utilized in the context of this study include current wetland areas (1973-2015) for 'Mangrove forests'[34], 'Salt marshes'[35] and 'Tidal freshwater marshes'[53]. Based on a literature search for the lower and upper elevation limits of mangroves, salt marshes and tidal freshwater marshes[53-57], we assume that all coastal wetland types are located at elevations between MSL and MHWS and can occur over the entire elevation range. The reported wetland areas for each coastline segment are distributed alongside the non-wetland floodplain on the previously constructed coastal profile (ED Fig.5). We appreciate that in nature, the upper and lower boundaries of coastal wetlands will vary as a result of different vegetation species, tidal currents and waves[59], but for our global application MSL as the lower, and MHWS as the upper, limit constitute solid boundaries.

Regional relative sea level rise data and scenarios

We use three SLR scenarios, covering the range of global SLR as projected by the IPCC AR5[45] plus a possible greater contribution of ice-sheets as assessed on the basis of post-AR5 methods[32]. The three scenarios represent the three representative concentration pathways (RCPs) 2.6, 4.5, and 8.5, paired with a low, medium and high ice-sheet contribution respectively, and generated using the general circulation model HadGEM2-ES[60] (ED Table2). The employed SLR scenarios are regionalized, therefore accounting for regional gravitational and rotational effects due to changes in ice mass distribution and steric variation[32]. Local relative SLR information is attained by combining the regionalized SLR projections with segment-specific vertical land movement based on a global model of glacial isostatic adjustment (GIA)[61] and some additional 2 mm yr^{-1} of natural subsidence in large river deltas[62,63] (ED Fig.6). Meanwhile, human-induced subsidence, which may be of particular importance in large river deltas[64], is not considered for calculating regional relative SLR. However, a sensitivity analysis using a delta-wide subsidence rates of 5 mm yr^{-1} showed only small deviation in overall global wetland areas (ED Table4). Tectonic and neotectonic uplift/subsidence processes, other than GIA, are also not included due to the lack of an appropriate global dataset.

Tidal range data

In order to calculate the WAS (ED Fig.4) and compute the vertical wetland extent within each coastline segment, we use a newly developed global tidal range dataset[65], representing the segment-specific mean low water (MLW), mean high water (MHW), mean high water neap (MHWN) and mean high water spring (MHWS) tidal levels. The new tidal dataset was generated using OTISmpi[66], a forward global tidal model, solving the non-linear shallow water equations on a C-grid using a finite differences time stepping method (Supplementary Information).

Population density

For each coastline segment, the coastal population within each elevation increment is computed by superimposing the SRTM digital elevation model[47] with the Global Rural-Urban Mapping Project (GRUMP) population data[67], being subject to national population growth according to SSP2 (IIASA)[20,68]. To determine the population density in the floodplain of the 1-in-100 year extreme water level, which is used as a proxy for the availability of accommodation space (ED Fig.4), we derive the hydrologically connected floodplain area for the 1-in-100 year extreme water level and the corresponding population affected by flooding[32]. We use the latest dataset on extreme water levels along the world's coastline, produced with a new global storm surge model hindcasting extreme water levels between 1979 and 2014[50]. Extreme water levels are reported for the return periods of 1, 10, 100 and 1000 years and are derived from total water levels during storm surge events, thus including both tides and surges.

Sediment availability

Local sediment availability is derived from MERIS satellite data, processed in the framework of the Globcolour project *(*http://globcolour.info*)*. The data represent total suspended matter (TSM) in the water column and have been developed, validated, and distributed by ACRI-ST, France[69]*.* We use the monthly averages from April 2002 to April 2012 that have a horizontal resolution of 1/24°. A long-term average is calculated for every pixel, and an average value of all pixels located within a 4 km buffer of each coastline segment is used to represent the local sediment availability (mg l^{-1}).

Sea-level rise impacts on coastal wetlands

Conversion of terrestrial upland to coastal wetlands

With increasing sea levels, we allow coastal wetlands to migrate inland, a process that we understand as the establishment of wetland vegetation inland of its previous location, by raising the MHWS level along the coastal profile. Hence, former terrestrial upland areas are inundated and converted to coastal wetlands (ED Fig.5), based on elevation, where no human barriers are assumed to be present[36-39]. This modelling approach is supported by recent local-scale field studies for coastal salt marshes at the US east coast and in the Gulf of Mexico[69-74] and has previously been applied through various local-scale models, both for salt marshes and mangroves[75-79]. The establishment of coastal wetland vegetation in inundated upland areas is assumed to be associated with a response lag of five years, which is in line with evidence produced by recent wetland restoration studies[80-83]. However, the development of related wetland functions (such as biogeochemical functioning) may take more time[74,80].

For calculation of the converted upland areas, we assume the segment-specific wetland/non-wetland proportion to remain constant over time, whereby the non-wetland area within a coastline segment equals the total floodplain area (i.e. the total interpolated area between MSL and MHWS) minus the reported wetland area. The conversion of uplands to wetlands is therefore calculated as the product of the wetland/non-wetland proportion and the total inundated upland area. However, conversion of terrestrial upland to coastal wetland is assumed to be zero where the coastal population density within the floodplain of the 1-in-100 year extreme water level exceeds the given thresholds (5, 20, 150 or 300 people km^{-2}), representing the existence of anthropogenic barriers to inland wetland migration. We thereby assume that coastal protection infrastructure is an important contributor to anthropogenic barriers for wetland inland migration[2,8,36-39] and is built where coastal communities are threatened by extreme water levels, such as a 1-in-100 year event[32,84].

Seaward loss of coastal wetlands

As sea level rises, not only the upper wetland boundary (MHWS) but also the lower wetland boundary (MSL) shifts position, potentially causing inundation of coastal wetlands beyond physiological tolerance. Therefore, we calculate an “unconstrained seaward loss” which at first neglects the wetland’s capacity to vertically adapt to SLR by sediment accretion (Fig.ED2). Through sediment accretion, this unconstrained seaward loss may, however, be reduced or inhibited, given sufficient sediment availability within the coastline segment (ED Fig.4).

The Wetland Adaptability Score (WAS) is a measure for the difference between the sediment needed for the coastal wetland to vertically accrete sediment as fast as SLR and the sediment available. It represents a sediment surplus if positive, and a sediment deficit if negative (Fig. 3). The amount of sediment needed for a coastal wetland to adapt to SLR has been studied by Kirwan et al.[40], using an ensemble of five models for tidal marsh accretion. They present linear relationships between sediment availability and the maximum rate of relative SLR that a tidal marsh can survive, showing steeper slopes (higher resilience) for marshes in macrotidal environments compared to marshes in microtidal environments. We directly use these linear relationships for our tidal marshes (including tidal salt and freshwater marshes), whereas we modify the model parameters for modelling mangrove forests during our calibration procedure (Supplementary Information). The local sediment availability, as derived from the Globcolour data, is assumed to represent the current levels of TSM in the coastal zone and assumed to remain constant during the simulation period. To account for possible changes in future global sediment supply, a sensitivity analysis has been conducted with average sediment availability levels reduced and increased by 20% and 50% (ED Table3).

The WAS thus represents the ability of the coastal wetlands within a coastline segment to adapt to rising sea levels by sediment accretion. A positive WAS implies that sediment availability is sufficient to maintain the present wetland area whereas a negative WAS implies that coastal wetlands are inundated and (partially) lost in response to SLR. The WAS is an integer value that ranges from -5 to +5, indicating a very high (-5) to very low (-1) sediment deficiency and a very low (+1) to very high (+5) sediment surplus respectively. Based on the WAS (*WAS*), the unconstrained seaward loss (SL_{unc}: km^2) is transformed into a constrained seaward loss (SL_c: km^2), assuming a linear relationship between *WAS* and the proportion of inundated wetland actually being lost, but only if *WAS* is negative (eq. 1). No wetland loss is computed where *WAS* is positive or zero. With SLR both *WAS* and SL_{unc} change over time. Thus SL_c is updated after every time step (t_i).

$$SL_c(t_i)=(-1/5)*WAS(t_i)*SL_{unc}(t_i) \quad \text{(eq. 1)}$$

The calculation of *WAS* is based on the assumption that the critical rate of relative SLR ($RSLR_{crit}$: mm yr^{-1}) depends on sediment availability (*Sed*: mg l^{-1}) and tidal range (*TR*), as suggested by Kirwan et al.[40]. Their modelling results can be approximated using the following relationship (eq. 2):

$$RSLR_{crit}=(m*TR^{\wedge}e)*Sed+i \qquad \text{(eq. 2)}$$

where ($m*TR^{\wedge}e$) represents the slope of a linear relationship between $RSLR_{crit}$ and *Sed*. Model parameters *e*, *i* and *m* are calibrated separately for tidal marshes (including tidal salt and freshwater marshes, e_{TF}, i_{TF} and m_{TF}) and mangrove systems (e_{Man}, i_{Man} and m_{Man}). Parameters e_{TF}, i_{TF} and m_{TF} are directly derived from the model ensemble runs of Kirwan et al.[40] and e_{Man}, i_{Man} and m_{Man} are estimated by calibrating the model using the mangrove data presented by Lovelock et al.[1] (Supplementary Information).

To estimate the sediment needed for a given SLR rate, Sed_{crit} (mg l^{-1}), we rewrite equation 2 as follows (eq. 3):

$$Sed_{crit}=(RSLR-i)/(m*TR^e) \qquad \text{(eq. 3)}$$

where *RSLR* (mm yr^{-1}) is the actual (time dependent) local relative SLR rate. Knowing the current sediment availability (*Sed*) within each coastline segment (derived from the Globcolour data), we compare this value with the segment-specific Sed_{crit} and define *WAS* as the scaled and rounded difference between the available and needed sediment availability (eq. 4):

$$WAS=round((Sed-Sed_{crit})/a)*5) \qquad \text{(eq. 4)}$$

where *a* represents the sediment surplus (or deficit in case $sedsup < sedsup_{crit}$), which is considered as “very high”. The determination of *a* is subject to model calibration (Supplementary Information). All *WAS* values greater (smaller) than 5 (-5) are transformed to *WAS* values of 5 (-5).

Model calibration

The model parameters m_{TF}, m_{Man}, e_{TF}, e_{Man}, i_{TF}, i_{Man} and *a* (eqs. 3+4) are estimated using a stepwise calibration procedure as described in detail in the Supplementary Information. Model results are thereby compared to field measurements of vertical elevation growth for 39 marsh sites across US and European Atlantic shorelines[4], 18 marsh sites in North America, Europe and north-east Australia[3] and 26 mangrove sites across Pacific shorelines[3]. The calibrated model (m_{TF}=3.42, m_{Man}=4.42, e_{TF}=0.915, e_{Man}=1.18, i_{TF}=1.5, i_{Man}=0 and a=40 mg l^{-1}) correctly predicts whether there is a sediment deficit, a sediment surplus or a balanced sediment budget for 78% of the coastline segments where field data is available (ED Table1).

Scenarios

The three SLR scenarios RCP 2.6, 4.5 and 8.5, accounting for the full range of available SLR scenarios[45], are combined with three human adaption scenarios. These are subject to population growth according to SSP 2 (ED Table2) which is considered a middle-of-the-road scenario for population growth[68]. The three different human adaptation scenarios include a business-as-usual (BAU) scenario, a moderate nature-based adaptation scenario (NB 1) and an extreme nature-based adaptation scenario (NB 2). They reflect differences in the potential of coastal wetlands to migrate inland until 2100 due to potential differences in future coastal management strategies. In addition, four different physically and/or socio-economically unrealistic model configurations (ED Table2: hypothetical scenarios) were used during the sensitivity analysis to quantify the extent to which overall resilience is enabled/constrained by vertical and horizontal adaptability mechanisms, namely vertical sediment accretion and wetland inland migration.

Human adaptation scenarios

Inland/upward migration of coastal wetlands is often obstructed by the presence of anthropogenic infrastructure (e.g. dikes, seawalls, cities, roads, railways, etc.)[18,37]. As there is no global dataset on coastal infrastructure, we approximate accommodation space through a population density threshold above which we assume that no accommodation space is available for coastal wetlands to migrate inland/upward. We thereby assume that coastal infrastructure is more likely to be present, where population density is high[37,85], and that coastal protection structures are among the most important barriers for wetland inland migration[8]. By comparing a recent expert judgement on current coastal protection infrastructure, relying on population density and Gross National Income (GNI)[86], with coastal population densities within the 1-in-100 year extreme water level floodplain, we find that currently, on a global average, coasts of >20 people km^{-2} are protected by some kind of coastal protection infrastructure (Supplementary Information). We consider this number as the upper boundary of current accommodation space. This is because it only includes coastal protection infrastructure and neglects other anthropogenic infrastructure that may act as barrier. As a lower boundary we choose a population density threshold of 5 people km^{-2} as this has previously been used to define (nearly) uninhabited land[87]. We therefore define the range of threshold population densities between 5 and 20 people km^{-2} as our BAU scenario (Fig. 1 and ED Table2).

In two nature-based adaptation scenarios (NB 1 and NB 2) we assume that coastal societies in rural areas retreat from the coast with SLR, removing coastal protection and other infrastructure that inhibit inland migration of coastal wetlands. We thereby assume that this is more likely to happen in sparsely populated areas as compared to densely populated areas[8,88-90]. For the first nature-based adaptation scenario (NB 1), we assume an upper boundary of 150 people km^{-2} which corresponds to the OECD definition of urban areas[91]. In the second, more extreme nature-based adaptation scenario we use a threshold of 300 people km^{-2} as the upper boundary, since this corresponds to the European Commission's definition of urban areas[22] (ED Table2).

Hypothetical scenarios

The four hypothetical scenarios used for the sensitivity analysis include: (1) "wetland migration only", characterized by the exclusion of bio-physical vertical accretion mechanisms and unlimited inland accommodation space; (2) "sediment accretion only", characterized by the inclusion of bio-physical vertical accretion mechanisms, but assuming no inland accommodation space; (3) "maximum resilience", which includes bio-physical accretion mechanisms and assumes an unlimited potential for inland migration; and (4) "no resilience" where neither bio-physical accretion nor inland migration are accounted for (ED Table2).

It should be noted that these hypothetical scenarios are unrealistic from a socio-economic and/or physical perspective, since no future coast will be neither completely defended nor completely undefended by dikes and seawalls and neither will sediment accretion be fully absent. But these hypothetical model runs are meant to demonstrate the relative contributions of the two mechanisms of wetland inland migration and sediment accretion to the overall wetland resilience to SLR.

References

31 Vafeidis, A. T. *et al.* A new global coastal database for impact and vulnerability analysis to sea-level rise. *Journal of Coastal Research* **24**, 917-924 (2008).

32 Hinkel, J. *et al.* Coastal flood damage and adaptation costs under 21st century sea-level rise. *Proceedings of the National Academy of Sciences* **111**, 3292-3297 (2014).

33 Vafeidis, A. T. *et al.* Water-level attenuation in broad-scale assessments of exposure to coastal flooding: a sensitivity analysis. *Natural Hazards and Earth System Sciences Discussions*, doi:10.5194/nhess-2017-199 (2017).

34 Giri, C. *et al.* Status and distribution of mangrove forests of the world using earth observation satellite data. *Global Ecology and Biogeography* **20**, 154-159 (2011).

35 McOwen, C. *et al.* A global map of saltmarshes. *Biodiversity Data Journal* **5**, e11764 (2017).

36 Kirwan, M. L., Walters, D. C., Reay, W. G. & Carr, J. A. Sea level driven marsh expansion in a coupled model of marsh erosion and migration. *Geophysical Research Letters* **43**, 4366-4373 (2016).

37 Borchert, S. M., Osland, M. J., Enwright, N. M. & Griffith, K. T. Coastal wetland adaptation to sea level rise: Quantifying potential for landward migration and coastal squeeze. *Journal of Applied Ecology* (2018).

38 Gilman, E. L., Ellison, J., Duke, N. C. & Field, C. Threats to mangroves from climate change and adaptation options: A review. Aquatic Botany 89, 237-250 (2008).

39 Torio, D. D. & Chmura, G. L. Assessing Coastal Squeeze of Tidal Wetlands. *Journal of Coastal Research*, 1049-1061 (2013).

40 Kirwan, M. L. *et al.* Limits on the adaptability of coastal marshes to rising sea level. *Geophysical Research Letters* **37**, L23401 (2010).

41 D'Alpaos, A., Mudd, S. M. & Carniello, L. Dynamic response of marshes to perturbations in suspended sediment concentrations and rates of relative sea level rise. *Journal of Geophysical Research: Earth Surface* **116**, F04020 (2011).

42 French, J. Tidal marsh sedimentation and resilience to environmental change: Exploratory modelling of tidal, sea-level and sediment supply forcing in predominantly allochthonous systems. *Marine Geology* **235**, 119-136 (2006).

43 Kirwan, M. L. & Guntenspergen, G. R. Influence of tidal range on the stability of coastal marshland. *Journal of Geophysical Research: Earth Surface* **115**, F02009 (2010).

44 Temmerman, S., Govers, G., Wartel, S. & Meire, P. Modelling estuarine variations in tidal marsh sedimentation: response to changing sea level and suspended sediment concentrations. *Marine Geology* **212**, 1-19 (2004).

45 Church, J. A. *et al.* in *Climate Change 2013: The Physical Science Basis. Contribution of Working Group I to the Fifth Assessment Report of the Intergovernmental Panel on Climate Change* (T.F. Stocker *et al.*) 1137-1216 (Cambridge University Press, 2013).

46 McFadden, L., Nicholls, R. J., Vafeidis, A. & Tol, R. S. J. Methodology for modeling coastal space for global assessment. *Journal of Coastal Research* **23**, 911-920 (2007).

47 Jarvis, A., Reuter, H. I., Nelson, A. & Guevara, E. *Hole-Filled SRTM for the Globe Version 4*, Available online: http://srtm.csi.cgiar.org/ (2008).

48 Nicholls, R. J., Hoozemans, F. & Marchand, M. Increasing flood risk and wetland losses due to global sea-level rise: regional and global analyses. *Global Environmental Change* **9**, 69 - 87 (1999).

49 Nicholls, R. J. Coastal flooding and wetland loss in the 21st century: changes under the SRES climate and socio-economic scenarios. *Global Environmental Change* **14**, 69-86 (2004).

50 Muis, S., Verlaan, M., Winsemius, H. C., Aerts, J. C. J. H. & Ward, P. J. A global reanalysis of storm surges and extreme sea levels. *Nature Communication* **7** (2016).

51 Titus, J. G. & Richman, C. Maps of lands vulnerable to sea level rise modeled elevations along the US Atlantic and Gulf coasts. *Climate Research* **18**, 205-228 (2001).

52 Titus, J. G. & Wang, J. in *Background Documents Supporting Climate Change Science Program Synthesis and Assessment Product 4.1 (EPA 430R07004)* (eds J.G. Titus & E.M. Strange) (United States Environmental Protection Agency (EPA), 2008).

53 Vafeidis, A. T., Nicholls, R. J., McFadden, L., Hinkel, J. & Grasshoff, P. S. Developing a global database for coastal vulnerability analysis: design issues and challenges. *The International Archives of Photogrammetry, Remote Sensing and Spatial Information Sciences* **35**, 801-805 (2004).

54 Balke, T., Stock, M., Jensen, K., Bouma, T. J. & Kleyer, M. A global analysis of the seaward salt marsh extent: The importance of tidal range. *Water Resources Research* **52**, 3775-3786 (2016).

55 Ellison, J. in *Coastal Wetlands: An Integrated Ecosystem Approach* (eds. Perillo, E. Wolanski, D. Cahoon, & M. Brinson) 565-591 (Elsevier, 2009).

56 McIvor, A. L., Spencer, T., Möller, I. & M., S. *The response of mangrove soil surface elevation to sea level rise.* (The Nature Coservancy and Wetlands International 2013).

57 McKee, K. L. & Patrick, W. H. The relationship of smooth cordgrass (Spartina alterniflora) to tidal datums: a review. *Estuaries* **11**, 143-151 (1988).

58 Odum, W. E. Comparative ecology of tidal freshwater and salt marshes. *Annual Review of Ecology and Systematics* **19**, 147-176 (1988).

59 Gray, A. J., Marshall, D. F., Raybould, A. F., M. Begon, A. H. F. & Macfadyen, A. in *Advances in Ecological Research* Vol. 21 (eds. Begon, M., Fitter, A. & Macfadyen, A.) 1-62 (Academic Press, 1991).

60 Jones, C. D. *et al.* The HadGEM2-ES implementation of CMIP5 centennial simulations. *Geoscientific Model Development* **4**, 543 (2011).

61 Peltier, W. Global glacial isostasy and the surface of the ice-age earth: The ice-5G (VM2) model and grace. *Annual Review of Earth and Planetary Sciences* **32**, 111-149 (2004).

62 Meckel, T. A., Ten Brink, U. S. & Williams, S. J. Sediment compaction rates and subsidence in deltaic plains: numerical constraints and stratigraphic influences. *Basin Research* **19**, 19-31 (2007).

63 Syvitski, J.P.M. Deltas at risk. Sustainability Science **3**, 23-32 (2008).

64 Ericson, J. P., Vörösmarty, C. J., Dingman, S. L., Ward, L. G. & Meybeck, M. Effective sea-level rise and deltas: causes of change and human dimension implications. *Global Planetary Change* **50**, 63–82 (2006).

65 Pickering, M. D. *et al.* The impact of future sea-level rise on the global tides. *Continental Shelf Research* **142**, 50-68 (2017).

66 Egbert, G. D., Ray, R. D. & Bills, B. G. Numerical modeling of the global semidiurnal tide in the present day and in the last glacial maximum. *Journal of Geophysical Research: Oceans* **109**, C03003 (2004).

67 Center for International Earth Science Information Network - CIESIN - Columbia University, International Food Policy Research Institute - IFPRI, The World Bank & Centro Internacional de Agricultura Tropical - CIAT. *Global Rural-Urban Mapping Project, Version 1 (GRUMPv1): Population Density Grid*, Available online: http://dx.doi.org/10.7927/H4R20Z93 (2011).

68 Fricko, O. *et al.* The marker quantification of the Shared Socioeconomic Pathway 2: A middle-of-the-road scenario for the 21st century. *Global Environmental Change* **42**, 251-267 (2017).
69 Barrot, G., Mangin, A. & Pinnock, S. *Global Ocean Colour for Carbon Cycle Research, Product User Guide*. (ACRI-ST, 2007).
70 Raabe, E. A. & Stumpf, R. P. Expansion of Tidal Marsh in Response to Sea-Level Rise: Gulf Coast of Florida, USA. *Estuaries and Coasts* **39**, 145-157 (2016).
71 Schieder, N. W., Walters, D. C. & Kirwan, M. L. Massive Upland to Wetland Conversion Compensated for Historical Marsh Loss in Chesapeake Bay, USA. *Estuaries and Coasts* (2017).
72 Smith, J. A. M. The Role of Phragmites australis in Mediating Inland Salt Marsh Migration in a Mid-Atlantic Estuary. *PLOS ONE* **8**, e65091 (2013).
73 Langston, A. K., Kaplan, D. A. & Putz, F. E. A casualty of climate change? Loss of freshwater forest islands on Florida's Gulf Coast. *Global Change Biology* **23**, 5383-5397 (2017).
74 Anisfeld, S. C., Cooper, K. R. & Kemp, A. C. Upslope development of a tidal marsh as a function of upland land use. *Global Change Biology* **23**, 755-766 (2017).
75 Feagin, R. A., Martinez, M. L., Mendoza-Gonzalez, G. & Costanza, R. Salt marsh zonal migration and ecosystem service change in response to global sea level rise: a case study from an urban region. *Ecology and Society* **15**, 14 (2010).
76 Gilman, E., Ellison, J. & Coleman, R. Assessment of Mangrove Response to Projected Relative Sea-Level Rise And Recent Historical Reconstruction of Shoreline Position. *Environmental Monitoring and Assessment* **124**, 105-130 (2007).
77 Nitto, D. D. *et al.* Mangroves facing climate change: landward migration potential in response to projected scenarios of sea level rise. *Biogeosciences* **11**, 857-871 (2014).
78 Rogers, K., Saintilan, N. & Copeland, C. Managed Retreat of Saline Coastal Wetlands: Challenges and Opportunities Identified from the Hunter River Estuary, Australia. *Estuaries and Coasts* **37**, 67-78 (2014).
79 Stralberg, D. *et al.* Evaluating Tidal Marsh Sustainability in the Face of Sea-Level Rise: A Hybrid Modeling Approach Applied to San Francisco Bay. *PLOS ONE* **6**, e27388 (2011).
80 Craft, C., Broome, S. & Campbell, C. Fifteen Years of Vegetation and Soil Development after Brackish-Water Marsh Creation. *Restoration Ecology* **10**, 248-258 (2002).
81 Mossman, H. L., Brown, M. J. H., Davy, A. J. & Grant, A. Constraints on Salt Marsh Development Following Managed Coastal Realignment: Dispersal Limitation or Environmental Tolerance? *Restoration Ecology* **20**, 65-75 (2012).
82 Mossman, H. L., Davy, A. J. & Grant, A. Does managed coastal realignment create saltmarshes with ‘equivalent biological characteristics’ to natural reference sites? *Journal of Applied Ecology* **49**, 1446-1456 (2012).
83 Wolters, M., Garbutt, A., Bekker, R. M., Bakker, J. P. & Carey, P. D. Restoration of salt-marsh vegetation in relation to site suitability, species pool and dispersal traits. *Journal of Applied Ecology* **45**, 904-912 (2008).
84 Nicholls, R. J. *et al.* Stabilization of global temperature at 1.5°C and 2.0°C: implications for coastal areas. *Philosophical Transactions of the Royal Society A: Mathematical, Physical and Engineering Sciences* **376** (2018).
85 Song, J., Fu, X., Wang, R., Peng, Z.-R. & Gu, Z. Does planned retreat matter? Investigating land use change under the impacts of flooding induced by sea level rise. *Mitigation and Adaptation Strategies for Global Change* (2017).
86 Sadoff, C. W. *et al. Securing Water, Sustaining Growth: Report of the GWP/OECD Task Force on Water Security and Sustainable Growth.* (University of Oxford, 2015).
87 Mittermeier, R. A. *et al.* Wilderness and biodiversity conservation. *Proceedings of the National Academy of Sciences* **100**, 10309-10313 (2003).

88 Abel, N. *et al.* Sea level rise, coastal development and planned retreat: analytical framework, governance principles and an Australian case study. *Environmental Science & Policy* **14**, 279-288 (2011).
89 Kousky, C. Managing shoreline retreat: a US perspective. Climatic Change 124, 9-20 (2014).
90 Field, C. R., Dayer, A. A. & Elphick, C. S. Landowner behavior can determine the success of conservation strategies for ecosystem migration under sea-level rise. *Proceedings of the National Academy of Sciences* **114**, 9134-9139 (2017).
91 The Organisation for Economic Co-operation and Development - OECD. *OECD Regional Typology.* (OECD, 2011).

Code availability

The computer code that supports the findings of this study is available for non-commercial use (CC BY-NC-SA 4.0) from the GitLab repository "global-coastal-wetland-model", https://gitlab.com/mark.schuerch/global-coastal-wetland-model.git.

Data availability

The data that support the findings of this study are available from the corresponding author upon reasonable request. The source data for figures 1 and ED2 are provided with the paper.

Extended Data figure and table legends

ED Figure 1: Map of model performance during model calibration. Green lines indicate segments where the modelled sediment balances match the observed trends in wetland elevation change relative to sea level rise[3,4,19]. Red segments indicate model mismatches. The frequency distributions for total suspended matter (TSM) and tidal range (TR) display the distributions of both parameters in matching (green bars) and mismatching segments (red bars), and how they compare to the overall frequency distributions of both parameters (blue bars). The overall frequency distribution only includes coastline segments where coastal wetlands are present. The displayed coastline was generated during the DINAS-COAST FP5-EESD EU project (EVK2-CT-2000-00084).

ED Figure 2: Global change (km^2) in coastal wetland area. Results for all three SLR scenarios (RCP 2.6 - low, RCP 4.5 - medium, RCP 8.5 - high) and a total of eight different model configurations. These include the upper and lower boundaries of the BAU (5, 20 people km^{-2}) and the upper boundaries of the NB 1 and NB 2 scenarios (150 and 300 people km^{-2}) as defined in ED Table2 (solid lines). The dashed lines represent the four hypothetical scenarios, as characterized in ED Table2: (i) “wetland migration only”, (ii) “sediment accretion only”; (iii) “maximum resilience” and (iv) “no resilience”.

ED Figure 3: Spatial distribution of coastal wetland change. Absolute (a) and relative (b) changes in coastal wetland areas are displayed for a medium SLR scenario (RCP4.5 - med)), assuming the possibility of wetland inland migration everywhere, but in urban areas with a population density >300 people km^{-2}. Population density is subject the population growth throughout the simulation period, following the socio-economic pathway SSP2[20,68]. The displayed coastline was generated during the DINAS-COAST FP5-EESD EU project (EVK2-CT-2000-00084).

ED Figure 4: Flow diagram representing the overall structure of the global coastal wetland model. Input parameters are shown on the left, output parameters on the right. “Net wetland change” equals “Inland wetland gain” minus “Seaward wetland loss”.

ED Figure 5: Schematization of topographic profiles. The conversion of upland areas to coastal wetlands (if not inhibited by anthropogenic barriers) and the unconstrained seaward loss of coastal wetlands in response to sea level rise is shown for an exemplary coastline segment (in western France). Inundation of terrestrial uplands follows the rising mean high water spring (MHWS) level between the time steps t1 and t2 (blue), whereas the unconstrained seaward loss follows the increase in mean sea level (MSL) when neglecting sediment accretion processes (red). To improve the clarity of the figure the actual MHWS level (2.54 m) and MSL rise are exaggerated.

ED Figure 6: Map of regionalized relative sea level rise (m). Total relative sea level rise for the medium SLR scenario (ED Table2) during the simulation period, including a delta subsidence rate of 2 mm yr^{-1} (2010-2100). Black coastlines indicate regions of RLSR similar to the global mean. The displayed coastline was generated during the DINAS-COAST FP5-EESD EU project (EVK2-CT-2000-00084).

ED Table 1: Performance of calibrated model when compared to field data[3,4,19]. Summary of comparison between locally measured sediment balance[3,4] for marshes and mangrove systems[19] and modelled trends derived from the calculated WAS using m_{TM}=3.42, m_{Man}=4.42, iTF=1.5, i_{Man}=0, e_{TF}=0.915, e_{Man}=1.18 and a=40 mg l^{-1}. “Model fit” represents the number of segments, where the calculated WAS corresponds with the measured sediment category.

ED Table 2: Characteristics of the employed scenarios. Three sea level rise (SLR) scenarios (RCP 2.6 – low, RCP 4.5 – med, RCP 8.5 – high) were combined with three human adaptation scenarios (business-as-usual: BAU; moderate nature-based adaptation: NB 1; and extreme nature-based adaptation: NB 2), accounting for varying degrees of accommodation space available for coastal wetlands, and four hypothetical scenarios (HYS 1: wetland migration only, HYS 2: sediment accretion only, HYS 3: maximum resilience, HYS 4: no resilience), used to quantify the contribution of vertical sediment accretion and horizontal inland migration to the overall resilience of coastal wetlands to global SLR (sensitivity analysis).

ED Table 3: Model sensitivity to variations in sediment availability. Percent deviations in total global wetland area by 2100 from simulations with current-day sediment availability for all four population density thresholds (ED Table2) and reductions/increases of the constant sediment supply by 50% and 20%.

ED Table 4: Model sensitivity to variations in natural and human-induced delta subsidence. Percent gain (positive) and loss (negative) of total global wetland area by 2100 from simulations for all four population density thresholds (ED Table2) and three different rates for uniform delta subsidence for all 117 deltas listed in the DIVA database[31].

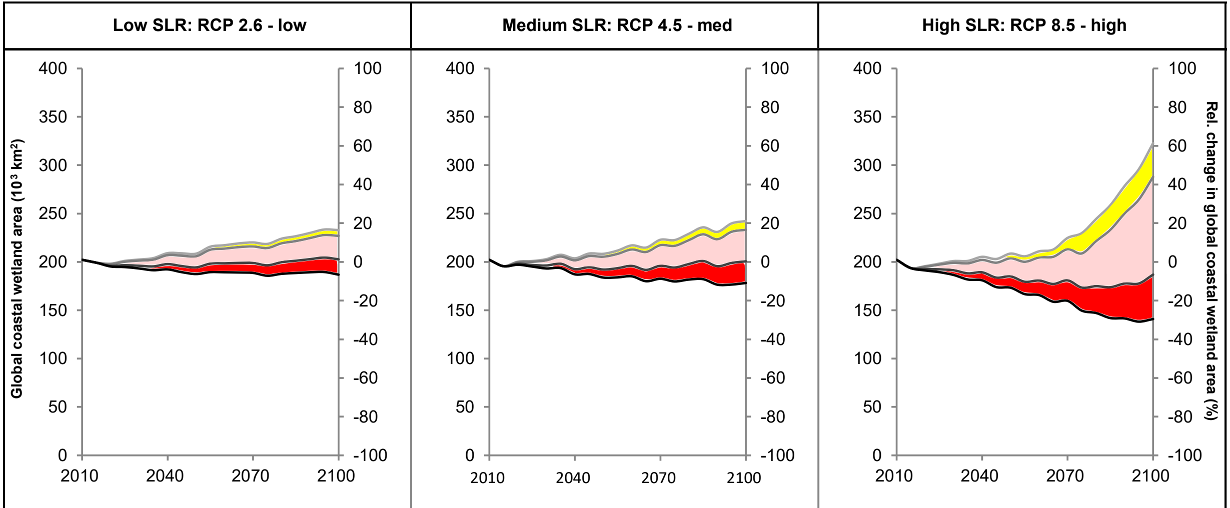

Pop. density threshold	Low SLR: Salt marsh change (km^2)	Low SLR: Freshw. marsh change (km^2)	Low SLR: Mangrove change (km^2)	Medium SLR: Salt marsh change (km^2)	Medium SLR: Freshw marsh change (km^2)	Medium SLR: Mangrove change (km^2)	High SLR: Salt marsh change (km^2)	High SLR: Freshw. marsh change (km^2)	High SLR: Mangrove change (km^2)
5	-871	-1,851	-12,645	-2,540	-1,517	-19,916	-5,994	-2,357	-52,862
20	4,770	-1,818	-2,455	4,046	-1,459	-4,149	4,685	-2,051	-17,923
150	9,872	1,573	13,318	10,828	786	19,415	18,438	-542	67,884
300	10,352	1,577	18,751	11,511	790	27,749	20,905	249	99,434

Pop. density threshold 5 — Pop. density threshold 20 — Pop. density threshold 150 — Pop. density threshold 300

Business-as-usual (BAU) — Natuere-based adpatation (NB) 1 — Nature-based adaptation (NB) 2

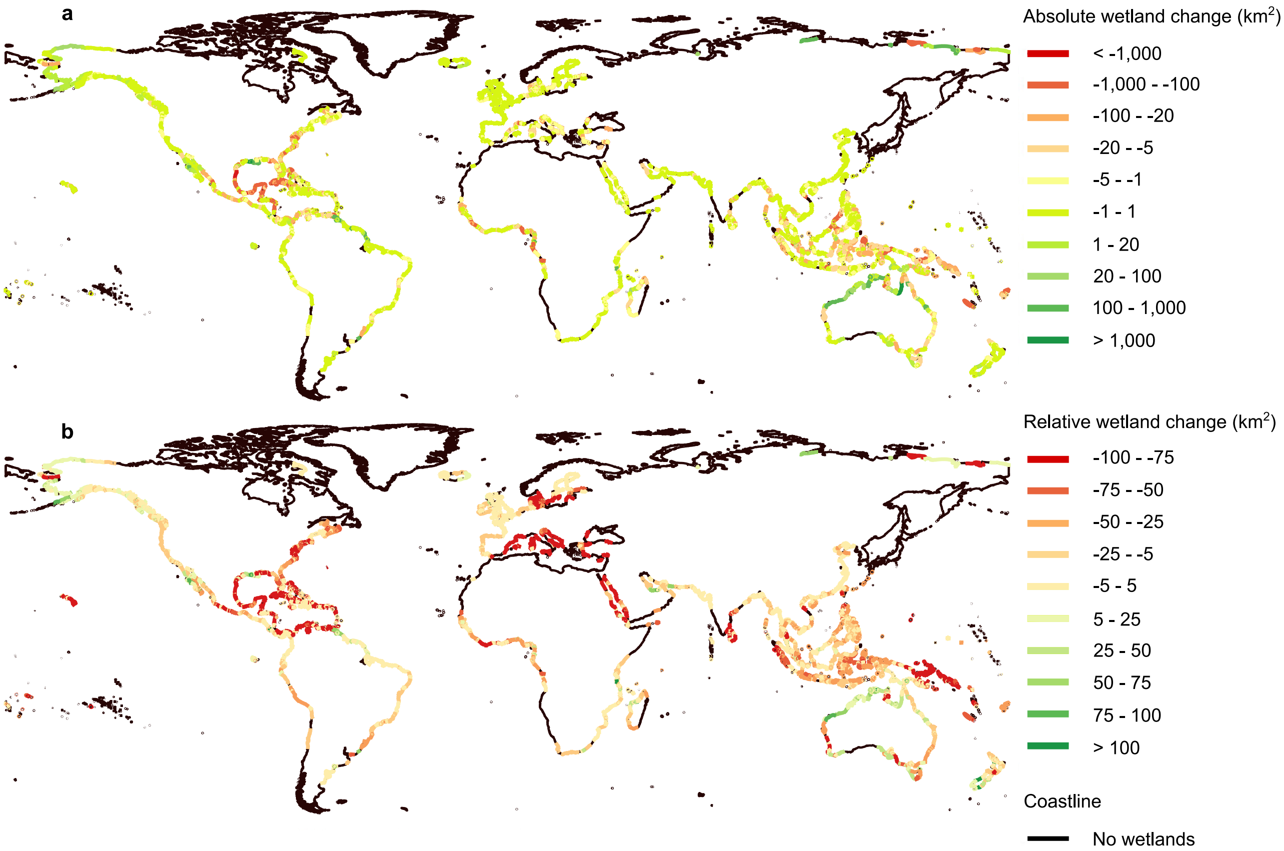
a
b
Absolute wetland change (km^2)
< -1,000
-1,000 - -100
-100 - -20
-20 - -5
-5 - -1
-1 - 1
1 - 20
20 - 100
100 - 1,000
> 1,000
Relative wetland change (km^2)
-100 - -75
-75 - -50
-50 - -25
-25 - -5
-5 - 5
5 - 25
25 - 50
50 - 75
75 - 100
> 100
Coastline
No wetlands

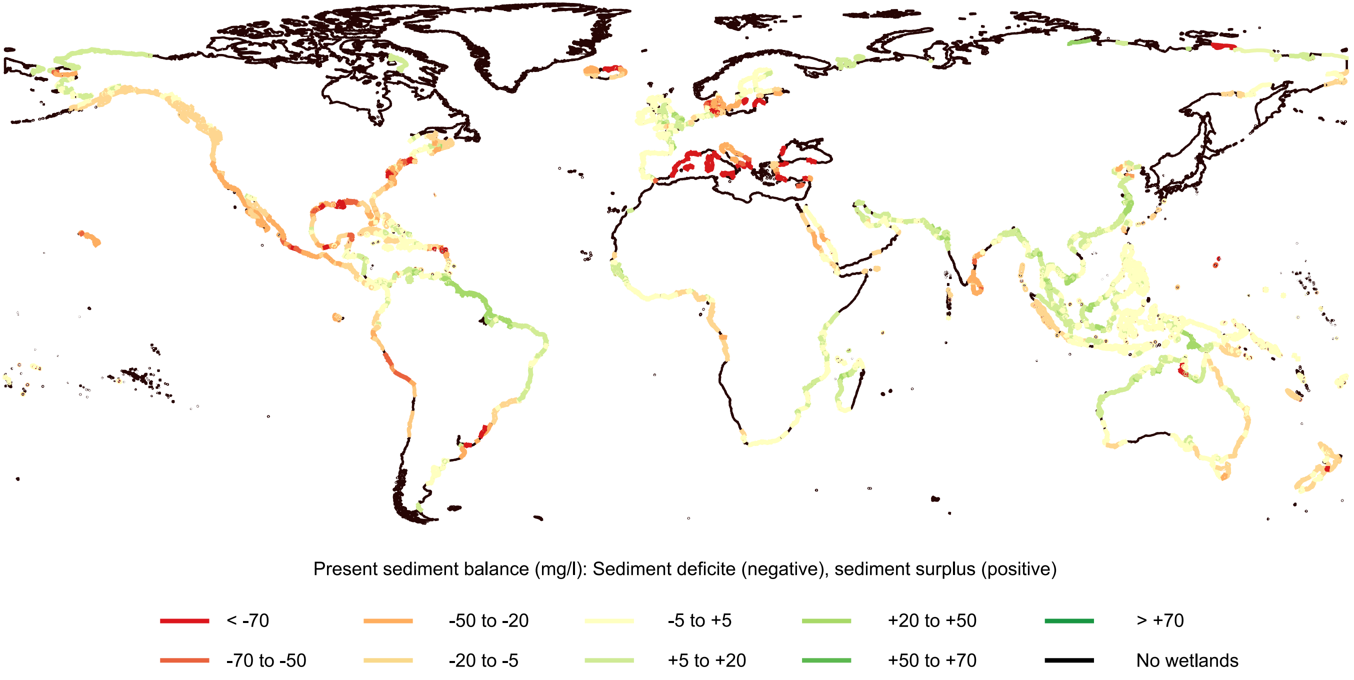
Present sediment balance (mg/l): Sediment deficite (negative), sediment surplus (positive)
< -70
-70 to -50
-50 to -20
-20 to -5
-5 to +5
+5 to +20
+20 to +50
+50 to +70
> +70
No wetlands

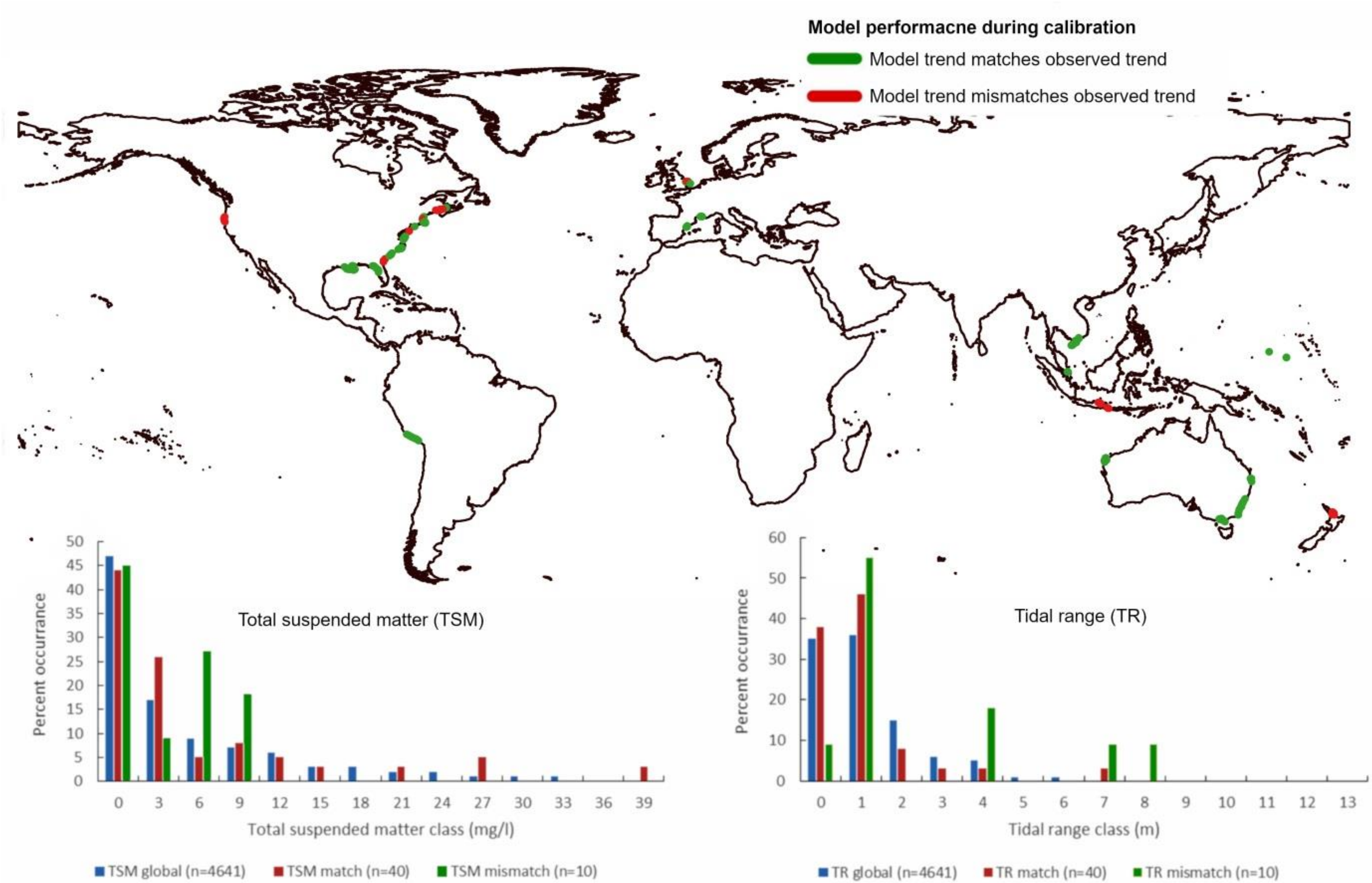

Model performacne during calibration
Model trend matches observed trend
Model trend mismatches observed trend
Total suspended matter (TSM)
Percent occurrance
0
5
10
15
20
25
30
35
40
45
50
0 3 6 9 12 15 18 21 24 27 30 33 36 39
Total suspended matter class (mg/l)
TSM global (n=4641)
TSM match (n=40)
TSM mismatch (n=10)
Tidal range (TR)
Percent occurrance
0
10
20
30
40
50
60
0 1 2 3 4 5 6 7 8 9 10 11 12 13
Tidal range class (m)
TR global (n=4641)
TR match (n=40)
TR mismatch (n=10)

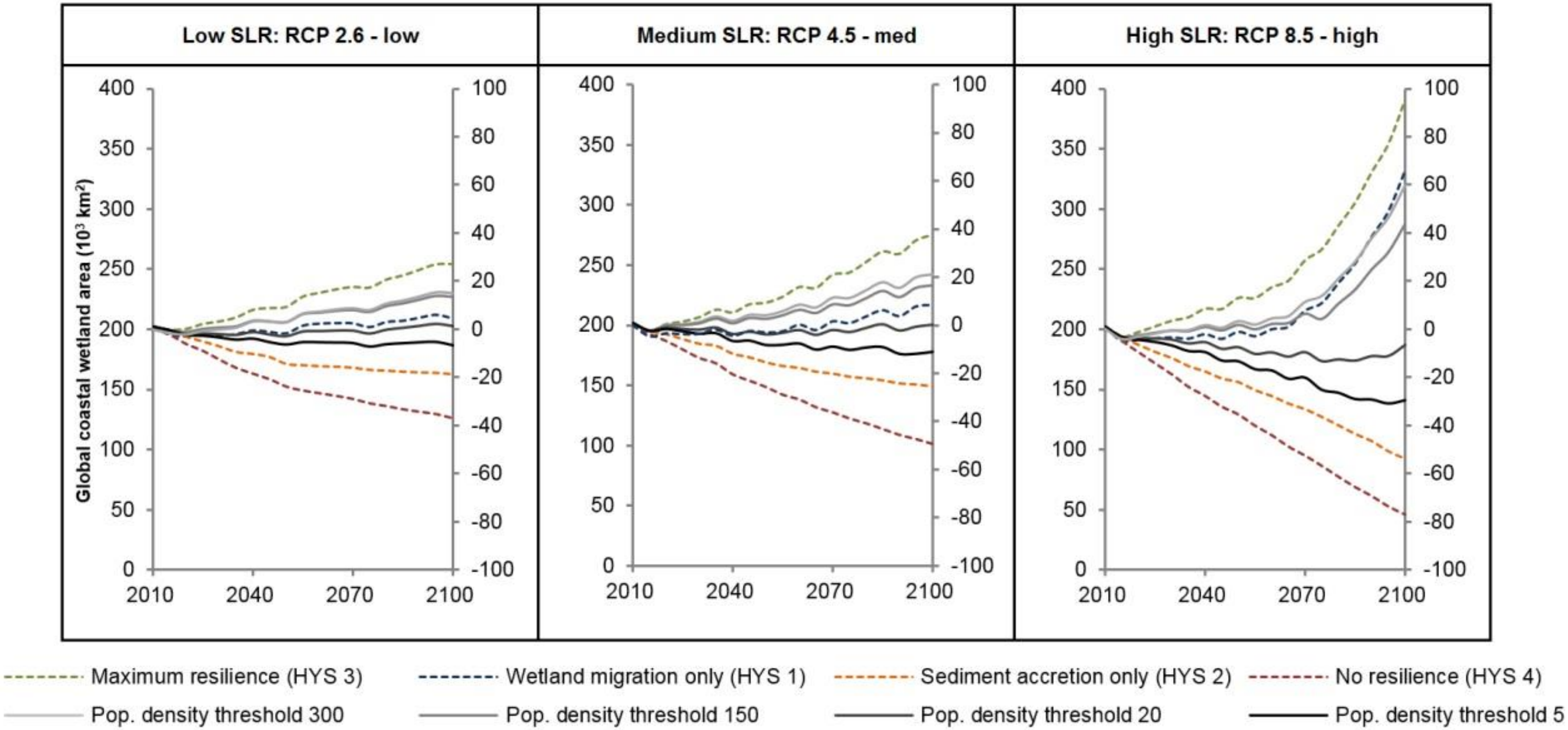
Low SLR: RCP 2.6 - low
Medium SLR: RCP 4.5 - med
High SLR: RCP 8.5 - high
Global coastal wetland area (10^3 km^2)
Maximum resilience (HYS 3)
Wetland migration only (HYS 1)
Sediment accretion only (HYS 2)
No resilience (HYS 4)
Pop. density threshold 300
Pop. density threshold 150
Pop. density threshold 20
Pop. density threshold 5

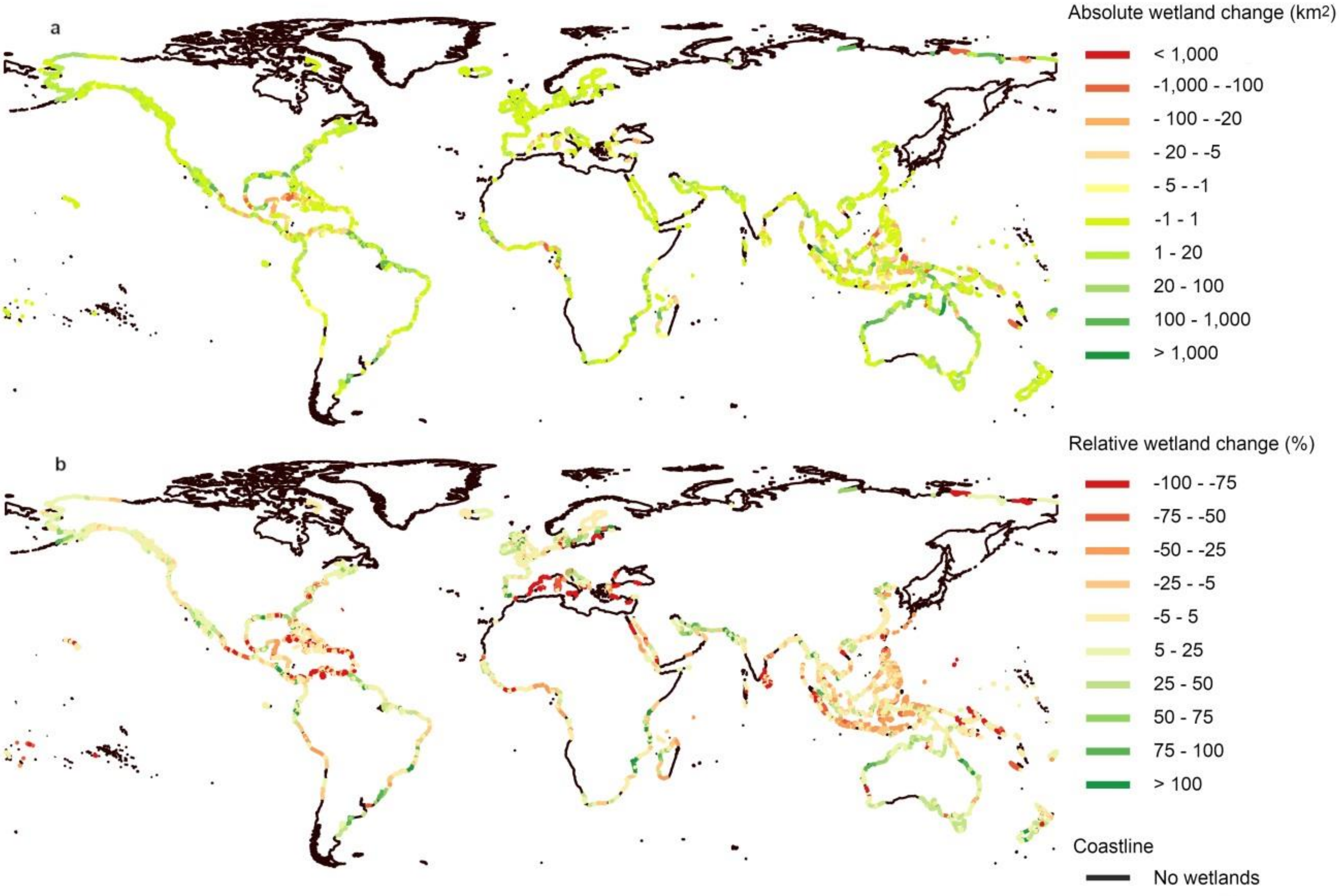
a
b
Absolute wetland change (km2)
< 1,000
-1,000 - -100
- 100 - -20
- 20 - -5
- 5 - -1
-1 - 1
1 - 20
20 - 100
100 - 1,000
> 1,000
Relative wetland change (%)
-100 - -75
-75 - -50
-50 - -25
-25 - -5
-5 - 5
5 - 25
25 - 50
50 - 75
75 - 100
> 100
Coastline
No wetlands

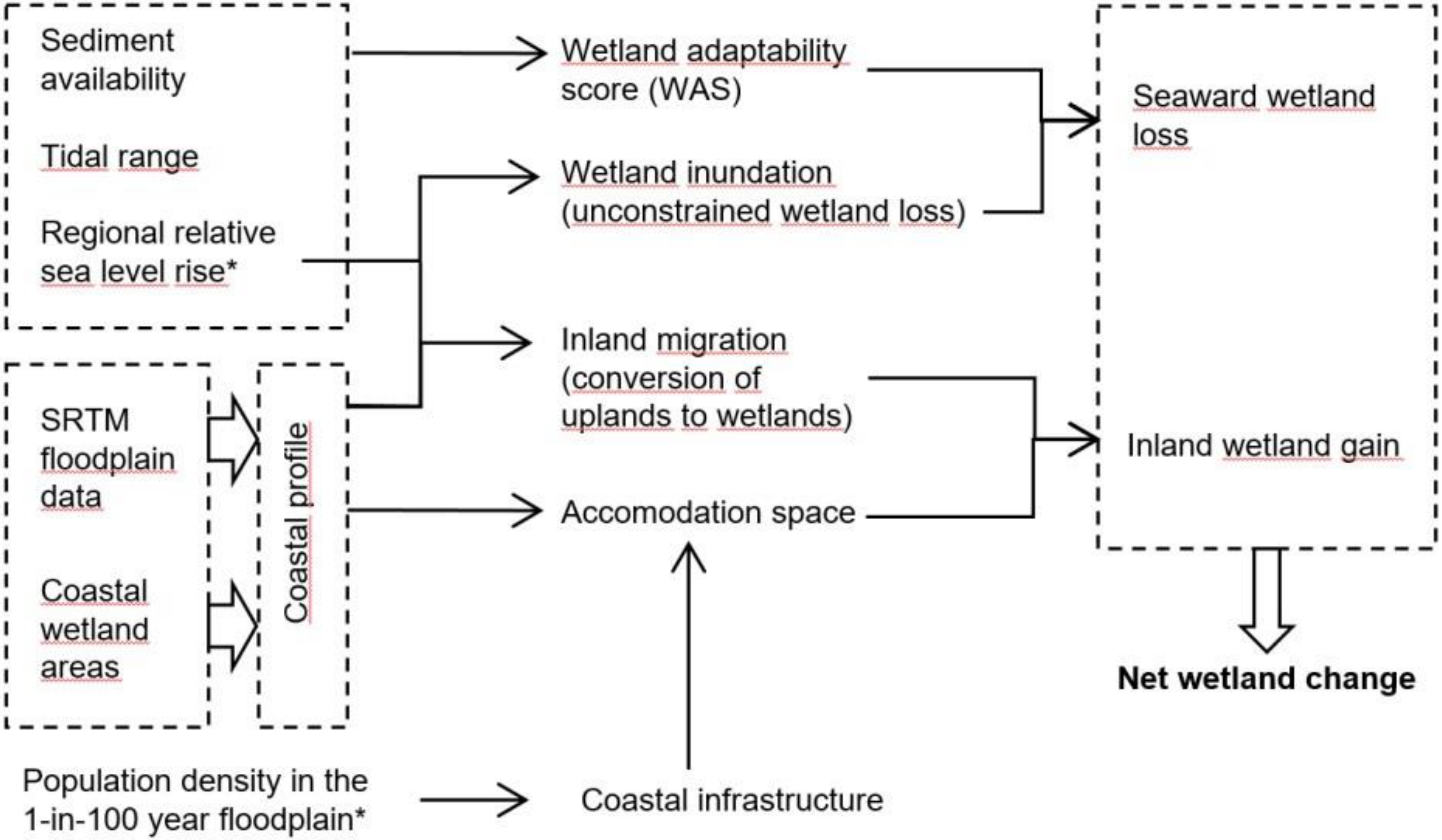

*Dynamic model variable, subject to projection until 2100

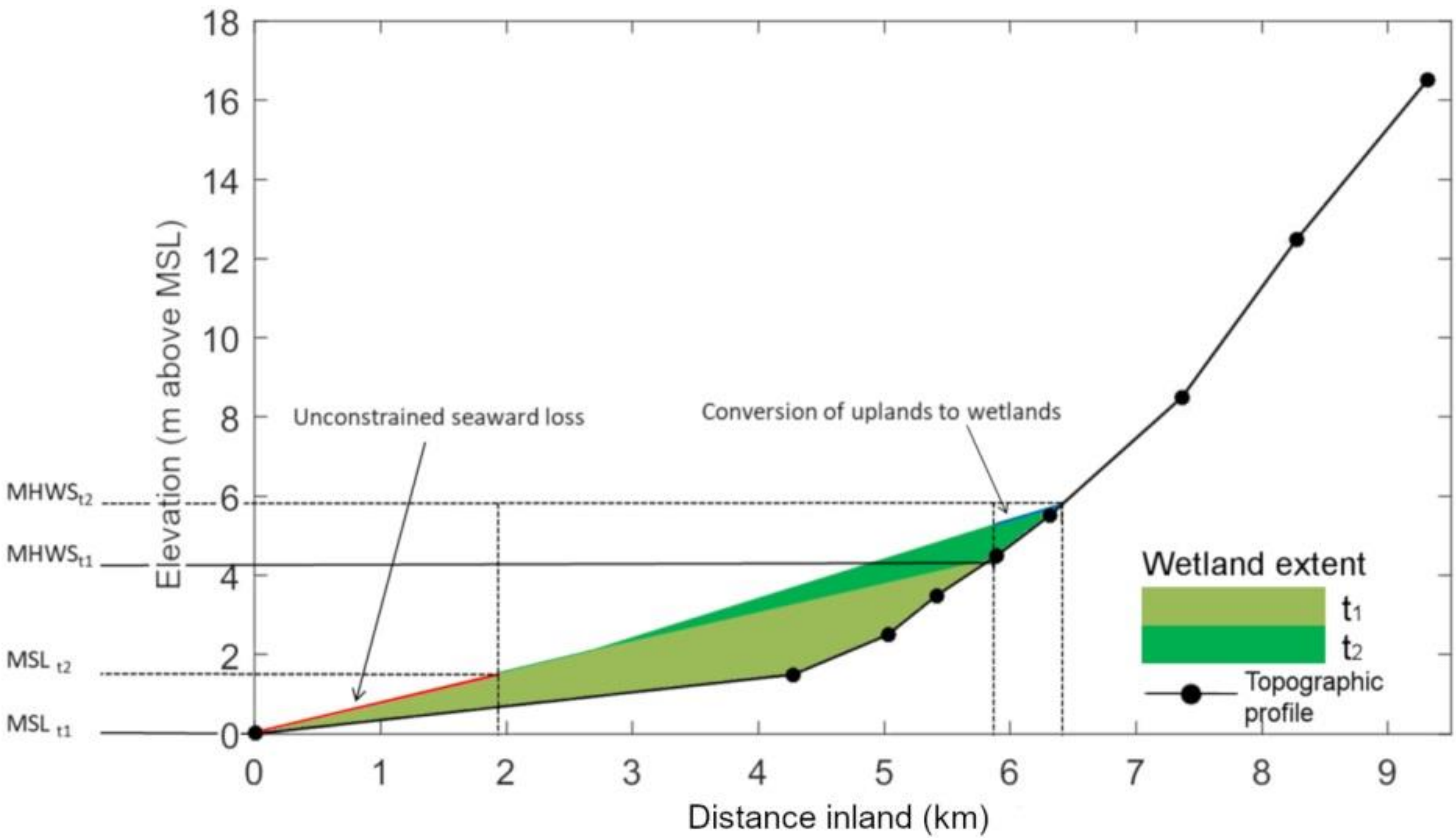

Unconstrained seaward loss
Conversion of uplands to wetlands
Elevation (m above MSL)
Distance inland (km)
MHWS t2
MHWS t1
MSL t2
MSL t1
Wetland extent
t1
t2
Topographic profile

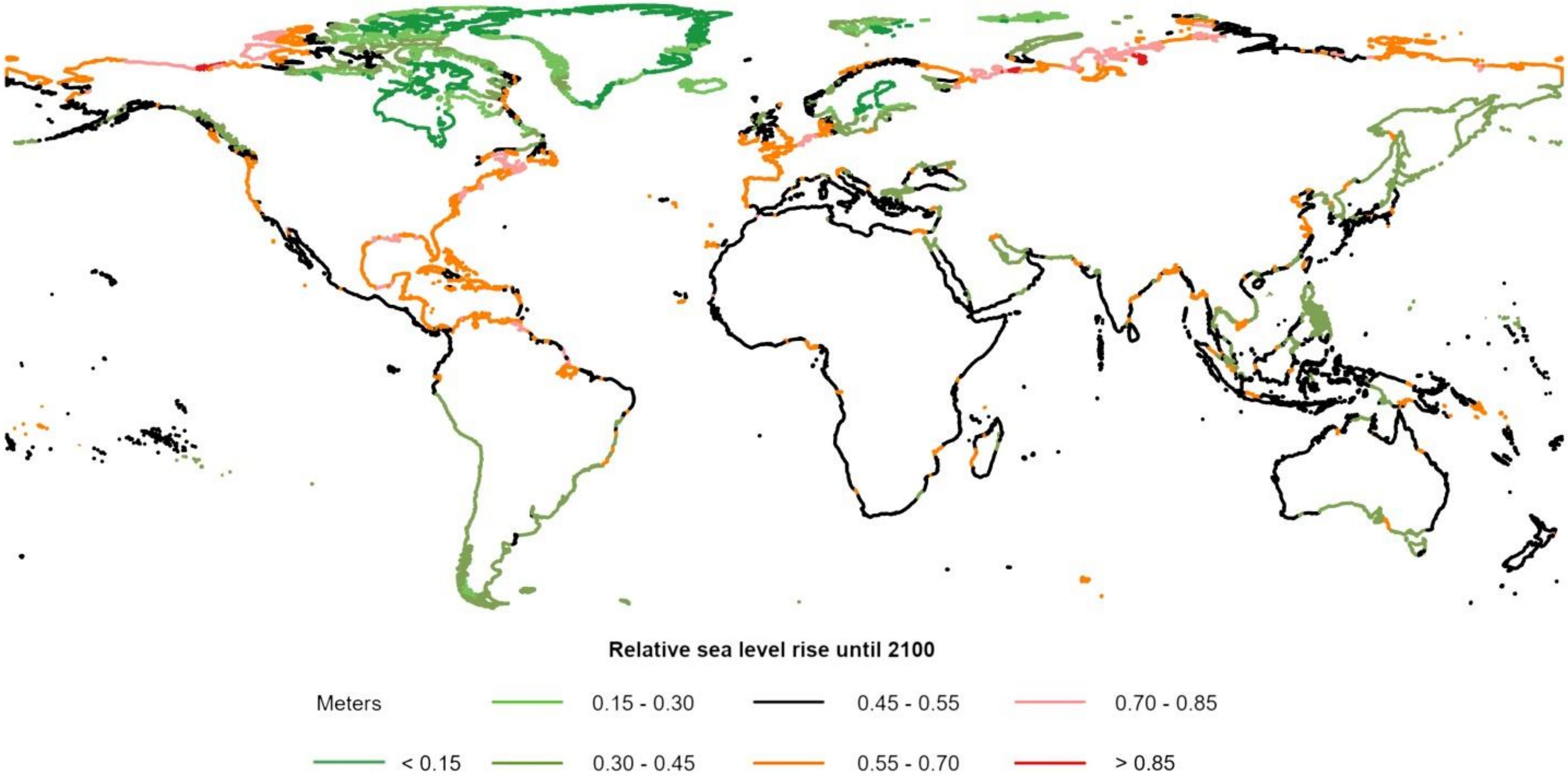
Relative sea level rise until 2100
Meters
< 0.15
0.15 - 0.30
0.30 - 0.45
0.45 - 0.55
0.55 - 0.70
0.70 - 0.85
> 0.85

	Category (defined based on the field measurements)	Categorization of Field measurements	WAS	Model fit (number of segments)	Total occurrences (number of segments)
Tidal marshes	Total model fit	All data	All data	16	23
	"elevation deficit"	< -2 mm yr^{-1}	<-1	3	5
	"balanced"	-2 to 2 mm yr^{-1}	-1 to 1	10	10
	"elevation surplus"	> 2 mm yr^{-1}	>1	3	8
Mangrove systems	Total model fit	All data	All data	20	23
	"elevation deficit"	< -2 mm yr^{-1}	<-1	12	12
	"balanced"	-2 to 2 mm yr^{-1}	-1 to 1	6	6
	"elevation surplus"	> 2 mm yr^{-1}	>1	2	5

SLR scenario	Land-ice contribution	SLR until 2100 (cm)	Accommodation space scenario		Scenario	Population density threshold (people km^{-2})		Sediment accretion
						Lower boundary	Upper boundary	
Low: RCP 2.6 (5%)	low	29	Human adaptation scenarios	BAU*	BAU	5	20	Yes
				NB†	NB 1	20	150	
				NB†	NB 2	150	300	
			4 Hypothetical scenarios (HYS)		HYS 1	∞‡	∞‡	No
					HYS 2	0§	0§	Yes
					HYS 3	∞‡	∞‡	Yes
					HYS 4	0§	0§	No
Medium: RCP 4.5 (50%)	medium	50	Human adaptation scenarios	BAU*	BAU	5	20	Yes
				NB†	NB 1	20	150	
				NB†	NB 2	150	300	
			4 Hypothetical scenarios (HYS)		HYS 1	∞‡	∞‡	No
					HYS 2	0§	0§	Yes
					HYS 3	∞‡	∞‡	Yes
					HYS 4	0§	0§	No
High: RCP 8.5 (95%)	high	110	Human adaptation scenarios	BAU*	BAU	5	20	Yes
				NB†	NB 1	20	150	
				NB†	NB 2	150	300	
			4 Hypothetical scenarios (HYS)		HYS 1	∞‡	∞‡	No
					HYS 2	0§	0§	Yes
					HYS 3	∞‡	∞‡	Yes
					HYS 4	0§	0§	No

*BAU: Business-as-usual scenario
†NB: Nature-based adaptation scenarios

‡Population density threshold = ∞: Unlimited accommodation space
§Population density threshold = 0: No accommodation space

Human adaptation scenario	Population density threshold (people km^{-2})	Sediment availability (constant in time)	RCP 2.6 - low (percent)	RCP 4.5 - medium (percent)	RCP 8.5 - high (percent)
Nature-based adaptation 2 – upper boundary	300	-50%	-2.9	-4.3	-6.5
		-20%	-1.1	-1.6	-2.5
		+20%	0.9	1.4	2.7
		+50%	2.5	3.5	6.1
Nature-based adaptation 2 – lower boundary = Nature-based adaptation 1 – upper boundary	150	-50%	-2.9	-4.3	-6.4
		-20%	-1.1	-1.6	-2.5
		+20%	0.9	1.4	2.7
		+50%	2.5	3.5	6.0
Nature-based adaptation 1 – lower boundary = Business-as-usual – upper boundary	20	-50%	-2.8	-4.1	-6.0
		-20%	-1.0	-1.5	-2.3
		+20%	0.9	1.3	2.5
		+50%	2.3	3.4	5.7
Business-as-usual – lower boundary	5	-50%	-2.7	-3.9	-5.7
		-20%	-1.0	-1.4	-2.2
		+20%	0.9	1.3	2.3
		+50%	2.3	3.3	5.3

Model setup	Delta subsidence (mm yr^{-1})	RCP 2.6 - 5% (percent)	RCP 4.5 - 50% (percent)	RCP 8.5 - 95% (percent)
Pop. density threshold 300	**0**	14.0	18.7	55.8
Pop. density threshold 150		11.4	14.8	39.5
Pop. density threshold 20		0.1	-1.0	-10.2
Pop. density threshold 5		-6.7	-10.6	-31.3
Pop. density threshold 300	**2**	15.2	19.8	59.7
Pop. density threshold 150		12.3	15.3	42.4
Pop. density threshold 20		0.2	-0.8	-7.6
Pop. density threshold 5		-7.6	-11.9	-30.3
Pop. density threshold 300	**5**	16.7	21.5	62.7
Pop. density threshold 150		12.8	15.5	44.1
Pop. density threshold 20		0.5	1.2	-6.3
Pop. density threshold 5		-9.6	-14.6	-31.0

Mark Schuerch[1,2*], Tom Spencer[2], Stijn Temmerman[3], Matthew L. Kirwan[4], Claudia Wolff[5], Daniel Lincke[6], Chris J. McOwen[7], Mark D. Pickering[8], Ruth Reef[9], Athanasios T. Vafeidis[5], Jochen Hinkel[6,10], Robert J. Nicholls[11], Sally Brown[11]

[1] Lincoln Centre for Water and Planetary Health, School of Geography, University of Lincoln, Lincoln, United Kingdom
[2] Cambridge Coastal Research Unit, Department of Geography, University of Cambridge, Cambridge United Kingdom [3] Ecosystem Management Research Group, University of Antwerp, Antwerp, Belgium
[4] Virginia Institute of Marine Science, College of William and Mary, Gloucester Point, Virginia, USA
[5] Institute of Geography, Christian-Albrechts University of Kiel, Kiel, Germany
[6] Global Climate Forum, Berlin, Germany
[7] UN Environment World Conservation Monitoring Centre, Cambridge, United Kingdom
[8] Ocean and Earth Science, National Oceanography Centre, University of Southampton, Southampton, United Kingdom
[9] School of Earth, Atmosphere and Environment, Monash University, Clayton, Victoria, Australia
[10] Division of Resource Economics, Thaer-Institute and Berlin Workshop in Institutional Analysis of Social-Ecological Systems (WINS), Humboldt-University, Berlin, Germany
[11] Faculty of Engineering and the Environment, University of Southampton, Southampton, United Kingdom

*Corresponding author: mschuerch@lincoln.ac.uk

<u>Future response of global coastal wetlands to sea level rise</u>

Supplementary Methods

The tidal range model

Our new tidal dataset[65,92] was generated using OTISmpi[66], a forward global tidal model, solving the non-linear shallow water equations on a C-grid using a finite differences time stepping method. The employed model setup is optimised to reconstruct shelf tides in order to assess tidal changes at major coastal port city locations around the world. The model outputs are comparable in accuracy to operational regional tidal models used to forecast tides and surge water levels at the coastline[65]. This purely physics based prognostic model setup was shown to have good skills at representing the present-day tides with an RMS error of 0.10 m globally, 0.21 m for shelf seas (<200 m) and 0.09 m in deep water (>200m)[92] when compared with the FES2004 tidal atlas solutions[93]. Additionally, as the prognostic model skill is not based on assimilation of any present-day observations, it can be used to assess changes to the tides with SLR and coastal adaptation.

OTISmpi was forced with the M2, S2, K1 and O1 dominant global tidal constituents and included iterative corrections for self-attraction and loading, as well as an internal wave drag parameterisation. The model was run for 50 days with the last 20 days used in the harmonic analysis to ensure that it had fully spun up and tidal constituents could be properly separated. All tidal parameters were derived from a 15-day sea-level reconstruction based on the four modelled tidal constituents; this time series included the spring HW peaks (semidiurnal regions) and tropical HW peaks (diurnal regions), it did not include longer term variability such as the equinoctial or nodal tides. MLW, MHWN and MHW were derived using a novel percentile method on the water level time series which enabled a spatially coherent field for these parameters across semidiurnal, diurnal and mixed tidal regimes[65,92]. The optimal percentiles derived were 10.8, 71.3 and 88.8 respectively with the mean taken of values +/-1%ile around each to provide a smooth field. Given the constituents used in the time series reconstruction, its length and the variety of tidal regimes the best method to estimate MHWS was to take the maximum of the 15-day time series.

The gridded tidal data (1/8° x 1/8°) was projected to each coastline segment by calculating the average of all grid cells intersecting the segment. If no grid cells crossed a segment (which is common around semi-enclosed seas), the nearest neighbour method was used. It should be noted that here we assume the tides to remain constant throughout the simulation period, although we acknowledge that SLR and coastal adaptation strategies, being dynamic variables within the model, may affect the tide itself[65].

Calibration procedure

The model parameters m, e, i and a (eqs. 3+4) are estimated using the following stepwise calibration procedure:

(i) Derivation of the coefficients m, i and e from the model ensemble runs presented by Kirwan et al.[40]. These coefficients are assumed to be valid for segments, where tidal marshes (tidal salt and freshwater marshes) are present and in the following referred to as m_{TM}, i_{TF} and e_{TF}.

(ii) Determination of model parameter a by comparing the modelled WAS with field measurements of elevation deficit/surplus on salt marshes derived from Sedimentation-Erosion Tables (SET), a widespread and standardized method for measuring the vertical elevation growth of coastal wetlands[94,95]. This dataset was compiled from meta-data analyses by Kirwan et al.[4] and Crosby et al.[3] and includes measurements of vertical marsh elevation changes from 57 marsh sites across Europe, Australia and North America. The majority of the data originates from the US East coast. We use the local RSLR rate reported by Kirwan et al.[4] and Crosby et al.[3] in combination with the tidal range data derived from Pickering et al.[92] to calculate the WAS for every coastline segment (eq. 3+4), where field measurements are available. Measured accretion deficits/surplus as well as the local RSLR rates are aggregated to the DIVA coastline segments by averaging all values within one segment.

The field measurements and the calculated WAS are divided into the three categories "sediment deficit", "balanced", "sediment surplus" (according to Suppl. Table 1) and the value of a in eq. 4 is changed such that the number of segments, where the model correctly estimates the measured category is maximized ("model fit").

(iii) Adoption of the model coefficients m_{TF}, e_{TF} *and* i_{TF} for mangrove systems. The model parameters are optimised by comparing the segment specific WAS, using the model parameter a, as determined in step (i), with the elevation change data presented by Lovelock et al.[19]. We thereby apply the exact same procedure as described in step (ii) except that m_{Man}, e_{Man} *and* i_{Man} are calibrated instead of a. In contrast to the model parameters m_{TF}, e_{TF} *and* i_{TF} the model parameters m_{Man}, e_{Man} *and* i_{Man} have to be calibrated against reported elevation data[19] as the ensemble model results by Kirwan et al.[40] are only applicable for tidal marshes, and no comparable study has been conducted for mangrove systems. Same as the data published by Kirwan et al.[4] and Crosby et al.[3], the data presented by Lovelock et al.[19] were assessed by SET measurements in 24 mangrove systems distributed across Southeast Asia and Australia.

The best model fit was achieved with m_{TM}=3.42, m_{Man}=4.42, i_{TF}=-1.5, I_{Man}=0, e_{TF}=0.915, e_{Man}=1.18 and a=40 mg l^{-1}. Suppl. Table 1 shows that during the final calibration run the model is well able to reproduce segments that are "balanced" or face a "sediment deficit", whereas the model performance in segments with a "sediment surplus" is lower. This bias implies that the model is more likely to underestimate the adaptive capacity of coastal wetlands, potentially resulting in an underestimation of the modelled global wetland areas.

Estimation of current-day coastal protection level

In order to define the population density thresholds for the upper and lower boundaries of our business-as-usual human adaptation scenario, which we assume to be representative of the current-day accommodation space of coastal wetlands, we define the population density threshold that corresponds to the proportion of the current-day coastline being protected by coastal sea defences as the upper limit. This assumption seems reasonable as inland migration of coastal wetlands is surely inhibited by coastal sea defences, but also by other coastal infrastructure, such as roads, railways and other impervious surfaces[18,96].

We therefore model the global distribution of coastal sea defences according the current state of the art and compare the percentage of globally protected coastline with the respective percentage, if the dike building decision in only based on local population density. The construction of coastal sea defences has been suggested to be related to the economic status of a region. Hinkel et al.[32], for example, use the national Gross Domestic Product (GDP) and population density to globally model the distribution of coastal sea defences. Similarly, Sadoff et al.[86] suggest protection levels to vary between poor and rich countries, with rich countries protecting sparser populated areas than poor countries. They suggest that countries with a Gross National Income (GNI) per capita of ≤$4085, defined as low and medium low-income countries by the United Nations[97], only protect their urban areas from coastal flooding, whereas richer countries (GNI per capita of >$4085) also protect their rural areas. While Sadoff et al.[86] do not give a definition for rural and urban, such definitions are given by the European Commission[22], who defines urban areas to be areas with population densities >300 people km^{-2}.

Under the assumption that the Gross Domestic Product (GDP) is comparable to the GNI[98,99], we use the GDP per capita and the population densities from Hinkel et al.[32] to model the global extent of coastal sea defences as suggested by Sadoff et al.[86]. We calculate the proportion of coasts globally that are protected by a coastal sea defence structure and compare this proportion with the corresponding proportion when modelling the extent of coastal sea defences using a range of population densities as a sole criteria (not considering GDP or GNI). The global proportion of protected coastline, using the GDP-population model by Sadoff et al.[86] is 41.97%. In comparison, the global proportion of protected coastline modelled with a population density threshold of 20 people km^{-2} (without considering GDP) is 41.90%. We therefore conclude that the present-day coastal protection level is best represented by a threshold population density of 20 people km^{-2}, which at the same time constitutes the upper boundary of our business-as-usual (BAU) scenario. For the lower boundary of the BAU scenario, we use a population density threshold of 5 people km^{-2}, below which no coastal sea defences are built, as these regions are considered (nearly) uninhabited[87].

Supplementary Discussion

Model limitations

We should emphasize that the model presented here is designed to predict the impacts of SLR on coastal wetland development, but does not account for changes in coastal wetland area due to anthropogenic conversion (i.e. land use change). With respect to socio-economic drivers we only consider the limitation of accommodation space, triggered by a (growing) coastal population (e.g. due to more coastal infrastructure). In the past, however, coastal wetland loss has widely been attributed to the conversion of coastal wetlands for agricultural, touristic and residential purposes[18,100].

While accounting for dynamic changes in SLR and coastal population, we assume other model parameters, such as tidal range, coastal topography or sediment availability to remain constant throughout the simulation period. Locally, temporal variability in these parameters may result in significantly different responses to what is suggested by our model. Furthermore, our sediment availability term is derived from long-term satellite data, delivering a pixel-specific long-term average with a horizontal resolution of 1/24°. These data cannot resolve local sediment dynamics on tidal mudflats, which may, however, significantly contribute to the overall sediment supply of a coastal wetland[101]. Furthermore, tidal mudflats in front of the vegetated tidal wetlands may also accrete sediment and grow vertically in time, hence allowing coastal wetlands to expand seawards. This process has been shown to be linked to the prevailing hydrodynamic conditions[102-104], but is not included in the presented model due to a lack of appropriate global-scale hydrodynamic data.

Being reliant on data that is available on a global scale, the processes represented within this model are strongly generalized and schematized, implying that locally and regionally, the morphological development of coastal wetlands may significantly deviate from the proposed model[59,102]. A lack of global data for the vertical evolution of coastal wetlands has also been highlighted by Webb et al.[105] who show that the available data is strongly biased towards North America, Europe and south-eastern Australia.

With respect to the calculation of the inland migration of coastal wetlands, we present a novel approach, whereby migration is calculated based on a schematization of a coastal profile, derived from SRTM data[47]. Conversion of dry upland areas to coastal wetlands is estimated using a bathtub style inundation model, which may overestimate the inundated areas as it does not take into account flow reduction due to surface roughness effects. The employed SRTM data have a vertical resolution of only 1 m, which makes it necessary to linearly interpolate between the different elevation increments. This method has previously been shown to allow for reliable impact modelling for SLR scenarios between 20 cm and 1 m (i.e. our scenarios are well within this range) despite the coarse vertical resolution of the SRTM data[51,52]. An attempt to quantify the error introduced by linear interpolation of elevation contours along the US east coast revealed a mean error of less than 30 cm and found that the interpolated elevation model was "as likely to overstate as understate the amount of land below a particular elevation"[52]. This independent finding shows the general suitability of linear interpolation for inundation modelling and delivers an estimate for the potential vertical error introduced by this methodology. However, locally, the coastal profile may significantly deviate from the assumption of a linear slope, thus influencing the inundation patterns. Moreover, in our approach we assume lower elevations to be located closer to the sea. This assumption has also been found to generally be representative of global coastal topography[33], but may locally lead to overestimation of wetland inland migration, if areas of low elevations (that are not hydrologically connected to the sea) are located further inland than higher elevations along the coast.

Additionally, inland migration of coastal wetlands or their ability to vertically adapt to global SLR may locally be affected by tectonic/neotectonic uplift or subsidence, respectively, as tectonic/neotectonic processes other than GIA are not considered in our model. However, on a global scale, we do not expect these processes to significantly affect the modelled wetland extents, as these processes uplift the coast in some regions, whilst lowering it in others. In contrast, human-induced subsidence in some of the large deltas of the world[63] exclusively trigger subsidence. This always increases RSLR and may locally reduce the ability of coastal wetland to vertically accrete with SLR. Wetland-internal variability in biophysical and biogeochemical processes (e.g. autocompaction[106], organic decomposition[107], internal waterlogging and vegetation die-off[108]) affecting the vertical performance of a coastal wetlands may also introduce a deviation of the assumed overall inland migration of a particular coastal wetland in response to global sea level rise.

References

92 Pickering, M. *The impact of future sea-level rise on the tides* (University of Southampton, (2014).

93 Lyard, F., Lefevre, F., Letellier, T. & Francis, O. Modelling the global ocean tides: modern insights from FES2004. *Ocean Dynamics* **56**, 394-415 (2006).

94 Boumans, R. M. J. & Day, J. W. High precision measurements of sediment elevation in shallow coastal areas using a sedimentation-erosion table. *Estuaries* **16**, 375-380 (1993).

95 Cahoon, D. R., Reed, D. J. & Day, J. W. Estimating shallow subsidence in microtidal salt marshes of the southeastern United States: Kaye and Barghoorn revisited. *Marine Geology* **128**, 1-9 (1995).

96 Carol, E., Kruse, E. & Tejada, M. Surface water and groundwater response to the tide in coastal wetlands: Assessment of a marsh in the outer Río de la Plata estuary, Argentina. *Journal of Coastal Research* **SI65**, 1098-1103 (2013).

97 United Nations. *World Economic Situation and Prospects 2014*. (United Nations, 2014).

98 OECD. *Gross national income (indicator)*, Available online: https://data.oecd.org (2017).

99 OECD. *Gross domestic product (indicator)*, Available online: https://data.oecd.org (2017).

100 Marcoe, K. & Pilson, S.. Habitat change in the lower Columbia River Estuary, 1870-2009. *Journal of Coastal Conservation* **21**, 505-525 (2017).

101 Schuerch, M., Dolch, T., Reise, K. & Vafeidis, A. T. Unravelling interactions between salt marsh evolution and sedimentary processes in the Wadden Sea (southeastern North Sea). *Progress in Physical Geography* **38**, 691-715 (2014).

102 Balke, T., Herman, P. M. J. & Bouma, T. J. Critical transitions in disturbance-driven ecosystems: identifying Windows of Opportunity for recovery. *Journal of Ecology* **102**, 700-708 (2014).

103 Silinski, A., Fransen, E., Bouma, T. J., Meire, P. & Temmerman, S. Unravelling the controls of lateral expansion and elevation change of pioneer tidal marshes. *Geomorphology* **274**, 106-115 (2016).

104 Zhu, Z., Zhang, L., Wang, N., Schwarz, C. & Ysebaert, T. Interactions between the range expansion of saltmarsh vegetation and hydrodynamic regimes in the Yangtze Estuary, China. *Estuarine, Coastal and Shelf Science* **96**, 273-279 (2012).

105 Webb, E. L. *et al.* A global standard for monitoring coastal wetland vulnerability to accelerated sea-level rise. *Nature Climate Change* **3**, 458-465 (2013).

106 Allen, J. R. L. Morphodynamics of Holocene salt marshes: a review sketch from the Atlantic and Southern North Sea coasts of Europe. Quaternary Science Reviews **19**, 1155-1231 (2000).

107 Kirwan, M., Langley, J., Guntenspergen, G. R. & Megonigal, J. The impact of sea-level rise on organic matter decay rates in Chesapeake Bay brackish tidal marshes. Biogeosciences **10**, 1869-1876 (2013).

108 Alber, M., Swenson, E. M., Adamowicz, S. C. & Mendelssohn, I. A. Salt Marsh Dieback: An overview of recent events in the US. Estuarine, Coastal and Shelf Science **80**, 1-11 (2008).